

Research Article

A Mathematical Analysis on the New Fractal-Fractional Model of Second-Hand Smokers via the Power Law Type Kernel: Numerical Solutions, Equilibrium Points, and Sensitivity Analysis

S. Rezapour^{1,2}, S. Etemad¹, M. Sinan³, J. Alzabut^{4,5} and A. Vinodkumar⁶

¹Department of Mathematics, Azarbaijan Shahid Madani University, Tabriz, Iran

²Department of Medical Research, China Medical University Hospital, China Medical University, Taichung, Taiwan

³School of Mathematical Sciences, University of Electronic Science and Technology of China, Chengdu 611731, China

⁴Department of Mathematics and Sciences, Prince Sultan University, Riyadh 11586, Saudi Arabia

⁵Department of Industrial Engineering, OSTİM Technical University, 06374 Ankara, Turkey

⁶Department of Mathematics, Amrita School of Engineering, Amrita Vishwa Vidyapeetham, Coimbatore 641112, India

Correspondence should be addressed to S. Etemad; sina.etemad@azaruniv.ac.ir

Received 10 December 2021; Accepted 25 March 2022; Published 10 May 2022

Academic Editor: Youssri Hassan Youssri

Copyright © 2022 S. Rezapour et al. This is an open access article distributed under the Creative Commons Attribution License, which permits unrestricted use, distribution, and reproduction in any medium, provided the original work is properly cited.

The second-hand smoke is a phenomenon that needs to be investigated, and its effects on the health of the people are to be examined. To analyze such an issue, the mathematical models are the best tools that help us to study the dynamical behaviors of this phenomenon. For this purpose, in the present paper, we consider a three-compartmental fractal-fractional mathematical model of a specific population of smokers or people that are exposed to second-hand smoke. By assuming some conditions on ϕ - ψ -contractions and compact operators, we prove some theorems in relation to the existence of solutions. The Banach principle for the usual contractions is used for proving the uniqueness of solutions. Next, by some notions of functional analysis, two types of Ulam-Hyers stability for the fractal-fractional second-hand smoker model are established. Moreover, we have a steady-state analysis and obtain equilibrium points and basic reproduction number R_0 . Then, we investigate the sensitivity of the fractal-fractional system with respect to each parameter. For numerical simulation, the Adams-Bashforth (AB) method is used to derive numerical schemes for plotting and simulating the approximate solutions. Finally, the obtained solutions are tested with real data and different values of fractal dimensions and fractional orders.

1. Introduction

The notion of the second-hand smoke is considered as the combination of smoke caused by the burning end of a cigarette, the smoke that is exhaled by a smoker, or smoke caused due to other tobacco products [1]. Therefore, being in the exposure of second-hand smoke, it involves an unintentional inhalation of smoke that happens near the people smoking or inhalation in an indoor environment where tobacco has been recently used. The people may be exposed to the second-hand smoke in different places that includes public places, home, private or public transport, workplace, home of relatives, and buses [2, 3]. Nowadays, the exposure

to second-hand smoke is considered one of the main risk factor for a class of diseases and harmful health-related results at a vast scale and is evaluated to cause more than 600,000 deaths in each year.

There exists an apparent relation between the factor of the second-hand smoke and an increased danger of stroke. Being in exposure to the second-hand smoke regularly in some public environment increases the chance of stroke by fifty percent [4]. At the same time, the second-hand smoke is as damaging to a fetus as if the mothers were inhaling the smoke directly from a cigarette [5]. Only 30 minutes of exposure to second-hand smoke can result in heart diseases similar to that of habitual smokers [6]. In view of these

items, being in exposure to second-hand smoke is regarded a subject of great concern for all of the people due to its familiar harmful effects on the human health.

Some of researchers have discussed about the adverse effects of second-hand smoke on the health problem as well. In 2011, Lubick et al. [7] conducted a research on the global health burden of the second-hand smoke, and in the same year, Burton [8] focused on an alarming consequence of smoking in indoor places. All the aforementioned studies indicate that the second-hand smoke is a significant problem worldwide.

The importance of this issue led to a number of researches being done in precise mathematical formats, because we have to model these phenomena to study their exact behaviors. Even during the recent years, researchers have modeled many phenomena and diseases by applying new mathematical operators and analyzed such systems numerically and analytically. Their findings help us to take steps about that specific disease and to control the speed of its spread. Instances of such a modeling can be found in [9, 10] by studying electrical circuits and some processes in engineering, in [11–14] for analyzing COVID-19, in [15, 16] for cancer treatment, in [17–19] for investigating different diseases, in [20–22] for controlling some viruses, in [23, 24] for studying some social problems, in [25, 26] for investigating some phenomena in relation to animals and agriculture, etc. More specifically, the operators with Mittag-Leffler-type kernels play an important role in recent mathematical modelings. To see these important phenomena, we can even enumerate some new works in this regard. Khan et al. [27] studied a fractional COVID-19 epidemic model with a convex incidence rate with the help of the Atangana-Baleanu operators in the Caputo sense and analyzed the optimal control on the amount of the infection. In [28], Akgul solved an Atangana-Baleanu fractional differential equation with the reproducing kernel Hilbert space method.

In this direction, the second-hand smoke is also a phenomenon which is important to investigate its effects based on mathematical models. To know some previous works about smoking models, Alkhudhari et al. [29] conducted a research on the global dynamics in relation to smoking on temporary quitters in 2014. One year later, Verma et al. [30] investigated a new model for the smoking cessation and the effects of media campaigns on this issue. Recently in 2019, Adhana et al. [31] studied a model of smoking tobacco in the form of a case study in Ethiopia and analyzed the smoking generation number (SGN) in relation to the given mathematical system. Pulecio-Montoya et al. [32] designed a model of the growth of tobacco consumers and simulated it by the fourth-order Runge-Kutta techniques.

In last decades, Atangana [33] introduced a new advanced kind of derivatives entitled fractal-fractional derivative that connects the two topics of fractional calculus and fractal calculus. Further, he extended the relevant fractal-fractional integral. The construction of such operators is in the form of the convolution of the power-law, exponential-law, and generalized Mittag-Leffler-law type kernels with fractal derivatives. Fractal-fractional operators have two

components: one is the fractional order and the second is the fractal dimension (order). Actually, differential equations furnished with the fractal-fractional derivative transfer the order and dimension of the supposed system into a rational order system.

According to this property, we can extend the usual differential equations to generalized systems with arbitrary order of derivatives and dimensions. In other words, the basic aim for defining these derivatives is to study nonlocal BVPs/IVPs in nature that contain fractal behaviors. In this direction, some mathematicians established several results and designed some fractal-fractional models that show better simulations for describing mathematical structures. For instance, Gomez-Aguilar et al. [34] analyzed the transmission of malaria with the help of these fractal-fractional operators. The situation and spread of coronavirus in Pakistan were studied in the form of a fractal-fractional model by Shah et al. in 2020 [35]. Also, one year later, Ali et al. developed another fractal-fractional model of COVID-19 based on the data extracted from Wuhan [36]. In [37], Farman et al. analyzed the solutions of a fractal fractional Atangana-Baleanu model of COVID-19 via the Atangana-Toufik scheme. In other paper, published by Amin et al. [38], the authors used the same fractal-fractional operators for investigating the effect of vaccination to control COVID-19. More recently, Alqhtani and Saad [39] used three types of fractal-fractional operators via the power-law, exponential decay, and Mittag-Leffler kernels for modeling Michaelis-Menten Enzymatic Reaction and compared their numerical results with the classical results. Also, Saad et al. [40] used the Caputo-Fabrizio fractal-fractional derivatives to model the hepatitis C virus infection and analyzed numerical solutions and their chaos with respect to different values of parameters.

In the present study, we will consider a three-compartmental mathematical model of a specific population of smokers or people that are exposed to second-hand smoke, and we will analyze and interpret our findings and model graphically, numerically, and analytically. Also, note that due to the importance of fixed point theory in proving the existence results, most of researchers use the main theorems of this field for confirming the existence of solutions for wide range of mathematical models. For instance, there are different theorems such as the Leray-Schauder fixed point theorem, Krasnoselskii's fixed point theorem [41], some fixed point theorems in partial metric spaces [42], or some special contractions such as F -contractions [43] and ϕ - ψ -contractions [44]. Here, we will use these new contractions for proving the existence of solutions.

We emphasize that the basic contribution and also the novelty of this work is that we compute and obtain our results based on a new model of second-hand smokers designed by the fractal-fractional derivatives for the first time. In the mentioned structure, we use power-law type kernel for this fractal-fractional derivative. Also, for the first time, to prove the existence of solutions, ϕ -admissible maps and ϕ - ψ -contractions play an important role in this study. Moreover, we try to investigate different stability results for the given model and at the end of the paper, we see that

our simulative graphs show the accuracy and applicability of the fractal-fractional operators in comparison to other usual fractional operators. Also, we again emphasize that this is the first work on the application of the fractal-fractional derivatives for modeling dynamics of second-hand smokers. The numerical and graphical results obtained in this work show that we can analyze different qualitative behaviors of mathematical models under the effect of the fractal dimension and fractional order of these new operators and obtain better and more accurate results with the help of real data. This confirms the considerable advantages of the fractal-fractional operators.

This model will be studied from several aspects. In the first place, after describing the suggested fractal-fractional model, we investigate existence theory based on two criteria in relation to ϕ - ψ -contractions and compact operators. The Banach principle for usual contractions is utilized for proving the uniqueness result. Next, by notions of functional analysis, two types of Ulam-Hyers stability of the fractal-fractional system are established. In the sequel, we have a steady-state analysis and obtain equilibria and reproduction number R_0 , and then we investigate the sensitivity of the fractal-fractional system with respect to each parameter. For numerical simulation, a fractional type of two-step Lagrange polynomial known as the fractional Adams-Bashforth (AB) method is utilized to derive numerical schemes for plotting and simulating the results. Finally, the obtained solutions are tested with real data and different values of fractal and fractional orders.

2. Preliminaries

In this section, we recall some definitions and properties on the fractal-fractional operators and some self-maps including ϕ - ψ -contractions.

We consider the family Ψ of all increasing functions $\psi : [0, \infty) \rightarrow [0, \infty)$ such that

$$\sum_{j=1}^{\infty} \psi^j(t) < \infty, \psi(t) < t, \forall t > 0. \quad (1)$$

Definition 1 (see [44]). Let $\mathcal{F} : \mathbb{X} \rightarrow \mathbb{X}$ and $\phi : \mathbb{X}^2 \rightarrow \mathbb{R}_{\geq 0}$, where \mathbb{X} is a normed space. Then,

(1) For $\mathcal{K}_1, \mathcal{K}_2 \in \mathbb{X}$, \mathcal{F} is ϕ - ψ -contraction if

$$\phi(\mathcal{K}_1, \mathcal{K}_2) d(\mathcal{F}\mathcal{K}_1, \mathcal{F}\mathcal{K}_2) \leq \psi(d(\mathcal{K}_1, \mathcal{K}_2)). \quad (2)$$

(2) \mathcal{F} is ϕ -admissible if

$$\phi(\mathcal{K}_1, \mathcal{K}_2) \geq 1 \implies \phi(\mathcal{F}\mathcal{K}_1, \mathcal{F}\mathcal{K}_2) \geq 1. \quad (3)$$

Definition 2 (see [33]). Let a continuous function $\mathcal{F} : (a, b) \rightarrow [0, \infty)$ be fractal differentiable of fractal order ν . Then, the fractal-fractional derivative of \mathcal{F} equipped with the

power-law-type kernel of order ω in the sense of Riemann-Liouville is defined by

$${}^{\text{FFP}}\mathfrak{D}_{a,t}^{\omega,\nu}\mathcal{F}(t) = \frac{1}{\Gamma(n-\omega)} \frac{d}{dt^\nu} \int_a^t (t-\mathfrak{w})^{n-\omega-1} \mathcal{F}(\mathfrak{w}) d\mathfrak{w}, \quad (4)$$

where $d\mathcal{F}(\mathfrak{w})/d\mathfrak{w}^\nu = \lim_{t \rightarrow \mathfrak{w}} ((F(t) - F(\mathfrak{w})) / (t^\nu - \mathfrak{w}^\nu))$ is the fractal derivative and $n-1 < \omega, \nu \leq n \in \mathbb{N}$.

One can simply observed that by letting $\nu=1$, the fractal-fractional derivative ${}^{\text{FFP}}\mathfrak{D}_{a,t}^{\omega,\nu}$ is the same standard Riemann-Liouville derivative ${}^{\text{RL}}\mathfrak{D}_{a,t}^\omega$ of order ω .

Definition 3 (see [33]). A continuous function \mathcal{F} defined on (a, b) is fractal-fractional integrable of the fractional and fractal orders ω and ν , respectively, via the power-law-type kernel if the integral

$${}^{\text{FFP}}\mathfrak{I}_{a,t}^{\omega,\nu}\mathcal{F}(t) = \frac{\nu}{\Gamma(\omega)} \int_a^t \mathfrak{w}^{\nu-1} (t-\mathfrak{w})^{\omega-1} \mathcal{F}(\mathfrak{w}) d\mathfrak{w} \quad (5)$$

exists, where $\nu, \omega > 0$.

3. Description of the Model for Second-Hand Smokers

This model of second-hand smoker tobacco involves a system of three differential equations [45]. The compartments are $\mathcal{P}(t)$, $\mathcal{S}(t)$, and $\mathcal{Q}(t)$. It is notable that $\mathcal{P}(t)$ represents the second-hand smokers or those (at risk of) exposure to others smoking, $\mathcal{Q}(t)$ denotes a group of persons who have cessation smoking but are at risk because of their previous smoking habit, and $\mathcal{S}(t)$ is a group of persons who are addicted to tobacco and smoke it yet. The variable as well as parameters used in the model is all nonnegative. Meaning of variables and parameters is given in the sequel. With the above assumptions, and based on [45], the second-hand smoker (SHS) model is provided by a system of ODEs in the form:

$$\begin{cases} \mathcal{P}'(t) = \theta - (s + q_1 + r)\mathcal{P}(t) - b\mathcal{S}(t)\mathcal{P}(t), \\ \mathcal{S}'(t) = b\mathcal{P}(t)\mathcal{S}(t) + r_1\mathcal{Q}(t)\mathcal{S}(t) - (q_1 + q_2 + r_2)\mathcal{S}(t), \\ \mathcal{Q}'(t) = r_2\mathcal{S}(t) - r_1\mathcal{S}(t)\mathcal{Q}(t) - (q_3 + q_1 + \gamma)\mathcal{Q}(t), \end{cases} \quad (6)$$

where θ is the number of healthful individuals who are also at risk of smoker people, q_1 stands for the natural mortality rate per total population, s is the death rate of second-hand smoker persons because of exposure to second-hand smoke, q_2 is the death rate of individuals by smoking tobacco, q_3 is the death rate of quit because of smoking habit before transferring to the phase \mathcal{Q} , r is the exit rate of second-hand smoker to the healthful individuals, γ is the exit rate of persons who have cessation smoking to the healthful people, b is the infection rate from \mathcal{P} to \mathcal{S} , r_2 is the exit rate from \mathcal{S} to \mathcal{Q} , and r_1 is the infection rate from \mathcal{Q} to \mathcal{S} . The limitations

for these parameters are $\theta > 0$, $0 < s \leq 1$, $0 < q_1 < 1$, and $0 \leq r, b, r_1, q_2, r_2, q_3, \gamma \leq 1$. The initial conditions are $\mathcal{P}(0) = \mathcal{P}_0 \geq 0$, $\mathcal{S}(0) = \mathcal{S}_0 \geq 0$, and $\mathcal{Q}(0) = \mathcal{Q}_0 \geq 0$.

Motivated by the above standard model, we here consider the fractal-fractional model of the second-hand smoker in the following structure:

$$\begin{cases} {}^{FFP}\mathfrak{D}_{0,t}^{\omega,\nu}\mathcal{P}(t) = \theta - (s + q_1 + r)\mathcal{P}(t) - b\mathcal{S}(t)\mathcal{P}(t), \\ {}^{FFP}\mathfrak{D}_{0,t}^{\omega,\nu}\mathcal{S}(t) = b\mathcal{P}(t)\mathcal{S}(t) + r_1\mathcal{Q}(t)\mathcal{S}(t) - (q_1 + q_2 + r_2)\mathcal{S}(t), \\ {}^{FFP}\mathfrak{D}_{0,t}^{\omega,\nu}\mathcal{Q}(t) = r_2\mathcal{S}(t) - r_1\mathcal{S}(t)\mathcal{Q}(t) - (q_3 + q_1 + \gamma)\mathcal{Q}(t), \end{cases} \quad (7)$$

subject to

$$\mathcal{P}(0) = \mathcal{P}_0 \geq 0, \mathcal{S}(0) = \mathcal{S}_0 \geq 0, \mathcal{Q}(0) = \mathcal{Q}_0 \geq 0, \quad (8)$$

where ${}^{FFP}\mathfrak{D}_{0,t}^{\omega,\nu}$ is the fractal-fractional derivative with the fractional order $\omega \in (0, 1]$ and the fractal order $\nu \in (0, 1]$ via the power-law-type kernel. We impose several required assumptions on the model: the parameters of (7) are nonnegative and

$$\mathcal{N}(t) = \mathcal{P}(t) + \mathcal{S}(t) + \mathcal{Q}(t), \quad (9)$$

where $\mathcal{N}(t)$ stands for the total population at the time $t \in \mathbb{I} := [0, T]$, ($T > 0$).

4. Existence of Solutions

In this section, the existence criterion is ensured by fixed point theory. Here, for the qualitative analysis, we define the Banach space $\mathbb{X} = \mathbb{M}^3$, where $\mathbb{M} = C(\mathbb{I}, \mathbb{R})$ under the norm

$$\|\mathbb{A}\|_{\mathbb{X}} = \|(\mathcal{P}, \mathcal{S}, \mathcal{Q})\|_{\mathbb{X}} = \max \{|\mathcal{K}(t)| : t \in \mathbb{I}\}, \quad (10)$$

for which $|\mathcal{K}| := |\mathcal{P}| + |\mathcal{S}| + |\mathcal{Q}|$. We rewrite the right-hand side of the fractal-fractional SHS-model (7) as

$$\begin{cases} \mathbb{W}_1(t, \mathcal{P}(t), \mathcal{S}(t), \mathcal{Q}(t)) = \theta - (s + q_1 + r)\mathcal{P}(t) - b\mathcal{S}(t)\mathcal{P}(t), \\ \mathbb{W}_2(t, \mathcal{P}(t), \mathcal{S}(t), \mathcal{Q}(t)) = b\mathcal{P}(t)\mathcal{S}(t) + r_1\mathcal{Q}(t)\mathcal{S}(t) - (q_1 + q_2 + r_2)\mathcal{S}(t), \\ \mathbb{W}_3(t, \mathcal{P}(t), \mathcal{S}(t), \mathcal{Q}(t)) = r_2\mathcal{S}(t) - r_1\mathcal{S}(t)\mathcal{Q}(t) - (q_3 + q_1 + \gamma)\mathcal{Q}(t). \end{cases} \quad (11)$$

Since, the integral is differentiable, we write the fractal-fractional SHS-model (7) in the following form:

$$\begin{cases} {}^{RL}\mathfrak{D}_{0,t}^{\omega,\nu}\mathcal{P}(t) = \nu t^{\nu-1}\mathbb{W}_1(t, \mathcal{P}(t), \mathcal{S}(t), \mathcal{Q}(t)), \\ {}^{RL}\mathfrak{D}_{0,t}^{\omega,\nu}\mathcal{S}(t) = \nu t^{\nu-1}\mathbb{W}_2(t, \mathcal{P}(t), \mathcal{S}(t), \mathcal{Q}(t)), \\ {}^{RL}\mathfrak{D}_{0,t}^{\omega,\nu}\mathcal{Q}(t) = \nu t^{\nu-1}\mathbb{W}_3(t, \mathcal{P}(t), \mathcal{S}(t), \mathcal{Q}(t)). \end{cases} \quad (12)$$

By (12), the developed system is illustrated by the following IVP

$${}^{RL}\mathfrak{D}_{0,t}^{\omega,\nu}A(t) = \nu t^{\nu-1}W(t, A(t)), \omega, \nu \in (0, 1], \quad (13)$$

where

$$\begin{aligned} A(t) &= (\mathcal{P}(t), \mathcal{S}(t), \mathcal{Q}(t))^T, A_0 = (\mathcal{P}_0, \mathcal{S}_0, \mathcal{Q}_0)^T, \\ W(t, A(t)) &= \begin{cases} \mathbb{W}_1(t, \mathcal{P}(t), \mathcal{S}(t), \mathcal{Q}(t)), \\ \mathbb{W}_2(t, \mathcal{P}(t), \mathcal{S}(t), \mathcal{Q}(t)), \\ \mathbb{W}_3(t, \mathcal{P}(t), \mathcal{S}(t), \mathcal{Q}(t)), t \in \mathbb{I}. \end{cases} \end{aligned} \quad (14)$$

Now, we operate on both sides of the Equation (13) by the fractal-fractional integral which is given by Definition 3, and we get

$$A(t) = A(0) + \frac{\nu}{\Gamma(\omega)} \int_0^t \mathfrak{w}^{\nu-1} (t - \mathfrak{w})^{\omega-1} W(\mathfrak{w}, A(\mathfrak{w})) d\mathfrak{w}. \quad (15)$$

In other words, the extended form of the above fractal-fractional integral is represented as

$$\begin{cases} \mathcal{P}(t) = \mathcal{P}_0 + \frac{\nu}{\Gamma(\omega)} \int_0^t \mathfrak{w}^{\nu-1} (t - \mathfrak{w})^{\omega-1} \mathbb{W}_1(\mathfrak{w}, \mathcal{P}(\mathfrak{w}), \mathcal{S}(\mathfrak{w}), \mathcal{Q}(\mathfrak{w})) d\mathfrak{w}, \\ \mathcal{S}(t) = \mathcal{S}_0 + \frac{\nu}{\Gamma(\omega)} \int_0^t \mathfrak{w}^{\nu-1} (t - \mathfrak{w})^{\omega-1} \mathbb{W}_2(\mathfrak{w}, \mathcal{P}(\mathfrak{w}), \mathcal{S}(\mathfrak{w}), \mathcal{Q}(\mathfrak{w})) d\mathfrak{w}, \\ \mathcal{Q}(t) = \mathcal{Q}_0 + \frac{\nu}{\Gamma(\omega)} \int_0^t \mathfrak{w}^{\nu-1} (t - \mathfrak{w})^{\omega-1} \mathbb{W}_3(\mathfrak{w}, \mathcal{P}(\mathfrak{w}), \mathcal{S}(\mathfrak{w}), \mathcal{Q}(\mathfrak{w})) d\mathfrak{w}. \end{cases} \quad (16)$$

To transform into a fixed point problem, we define $G : \mathbb{X} \longrightarrow \mathbb{X}$ by

$$G(A(t)) = A(0) + \frac{\nu}{\Gamma(\omega)} \int_0^t \mathfrak{w}^{\nu-1} (t - \mathfrak{w})^{\omega-1} W(\mathfrak{w}, A(\mathfrak{w})) d\mathfrak{w}. \quad (17)$$

In the preceding, we recall the required fixed point theorem in connection with our aim for proving the existence results.

Theorem 4 (see [44]). Assume that (\mathbb{X}, d) is a complete metric space, $\phi : \mathbb{X} \times \mathbb{X} \longrightarrow \mathbb{R}$, $\psi \in \Psi$, and $\mathbb{W} : \mathbb{X} \longrightarrow \mathbb{X}$ are an $\phi - \psi$ -contractive map such that

- (1) \mathbb{W} is ϕ -admissible self map on \mathbb{X}
- (2) For some $u_0 \in \mathbb{X}$, $\phi(u_0, \mathbb{W}u_0) \geq 1$
- (3) For any sequence $\{u_n\}$ in \mathbb{X} with $u_n \longrightarrow u$ and $\phi(u_n, u_{n+1}) \geq 1$ for all $n \geq 1$, we have $\phi(u_n, u) \geq 1$ for all $n \geq 1$

Then, there is a fixed point for \mathbb{W} .

Now, the first existence result is proved here under some special operators.

Theorem 5. Suppose that there are a map $h : \mathbb{R} \times \mathbb{R} \longrightarrow \mathbb{R}$, a continuous function $\mathbb{W} : \mathbb{I} \times \mathbb{X} \longrightarrow \mathbb{X}$, and a nondecreasing function $\psi \in \Psi$. Assume that

(\wp_1) For any $\mathbb{A}_1, \mathbb{A}_2 \in \mathbb{X}$ and $\mathbf{t} \in \mathbb{I}$,

$$|\mathbb{W}(\mathbf{t}, \mathbb{A}_1(\mathbf{t})) - \mathbb{W}(\mathbf{t}, \mathbb{A}_2(\mathbf{t}))| \leq \tilde{\ell} \psi(|\mathbb{A}_1(\mathbf{t}) - \mathbb{A}_2(\mathbf{t})|), \quad (18)$$

with $h(\mathbb{A}_1(\mathbf{t}), \mathbb{A}_2(\mathbf{t})) \geq 0$, where $\tilde{\ell} = \Gamma(\nu + \omega)/\nu T^{\nu+\omega-1}\Gamma(\nu)$.

(\wp_2) There is some $\mathbb{A}_0 \in \mathbb{X}$ such that for each $\mathbf{t} \in \mathbb{I}$,

$$h(\mathbb{A}_0(\mathbf{t}), G(\mathbb{A}_0(\mathbf{t}))) \geq 0, \quad (19)$$

and also the inequality

$$h(\mathbb{A}_1(\mathbf{t}), \mathbb{A}_2(\mathbf{t})) \geq 0 \quad (20)$$

gives

$$h(G(\mathbb{A}_1(\mathbf{t})), G(\mathbb{A}_2(\mathbf{t}))) \geq 0, \quad (21)$$

for each $\mathbb{A}_1, \mathbb{A}_2 \in \mathbb{X}$ and $\mathbf{t} \in \mathbb{I}$.

(\wp_3) For each convergent sequence $\{\mathbb{A}_n\}_{n \geq 1}$ that belongs to \mathbb{X} with $\mathbb{A}_n \longrightarrow \mathbb{A}$ and

$$h(\mathbb{A}_n(\mathbf{t}), \mathbb{A}_{n+1}(\mathbf{t})) \geq 0, \quad (22)$$

for each n and $\mathbf{t} \in \mathbb{I}$, we get

$$h(\mathbb{A}_n(\mathbf{t}), \mathbb{A}(\mathbf{t})) \geq 0. \quad (23)$$

Then, there is a solution for the fractal-fractional IVP (13), and so there is a solution to the given fractal-fractional SHS-model (7).

Proof. Let \mathbb{A}_1 and \mathbb{A}_2 be two members belonging to \mathbb{X} with

$$h(\mathbb{A}_1(\mathbf{t}), \mathbb{A}_2(\mathbf{t})) \geq 0, \quad (24)$$

for each $\mathbf{t} \in \mathbb{I}$. Then, by definition of the Beta function, we may write

$$\begin{aligned} |G(\mathbb{A}_1(\mathbf{t})) - G(\mathbb{A}_2(\mathbf{t}))| &\leq \frac{\nu}{\Gamma(\omega)} \int_0^t \mathbf{w}^{\nu-1} (\mathbf{t} - \mathbf{w})^{\omega-1} |\mathbb{W}(\mathbf{w}, \mathbb{A}_1(\mathbf{w})) \\ &\quad - \mathbb{W}(\mathbf{w}, \mathbb{A}_2(\mathbf{w}))| d\mathbf{w} \\ &\leq \frac{\nu}{\Gamma(\omega)} \int_0^t \mathbf{w}^{\nu-1} (\mathbf{t} - \mathbf{w})^{\omega-1} \tilde{\ell} \psi(|\mathbb{A}_1(\mathbf{w}) \\ &\quad - \mathbb{A}_2(\mathbf{w})|) d\mathbf{w} \\ &\leq \frac{\nu \tilde{\ell} T^{\nu+\omega-1} \mathbb{B}(\nu, \omega)}{\Gamma(\omega)} \psi(\|\mathbb{A}_1 - \mathbb{A}_2\|_{\mathbb{X}}) \\ &= \frac{\nu T^{\nu+\omega-1} \Gamma(\nu)}{\Gamma(\nu + \omega)} \tilde{\ell} \psi(\|\mathbb{A}_1 - \mathbb{A}_2\|_{\mathbb{X}}). \end{aligned} \quad (25)$$

Consequently, we have

$$\begin{aligned} \|G(\mathbb{A}_1) - G(\mathbb{A}_2)\|_{\mathbb{X}} &\leq \frac{\nu T^{\nu+\omega-1} \Gamma(\nu)}{\Gamma(\nu + \omega)} \tilde{\ell} \psi(\|\mathbb{A}_1 - \mathbb{A}_2\|_{\mathbb{X}}) \\ &= \psi(\|\mathbb{A}_1 - \mathbb{A}_2\|_{\mathbb{X}}). \end{aligned} \quad (26)$$

Now, a function $\phi : \mathbb{X} \times \mathbb{X} \longrightarrow [0, \infty)$ is introduced by the rule

$$\phi(\mathbb{A}_1, \mathbb{A}_2) = \begin{cases} 1 & \text{if } h(\mathbb{A}_1(\mathbf{t}), \mathbb{A}_2(\mathbf{t})) \geq 0, \\ 0 & \text{otherwise,} \end{cases} \quad (27)$$

for each $\mathbb{A}_1, \mathbb{A}_2 \in \mathbb{X}$. Then, for every $\mathbb{A}_1, \mathbb{A}_2 \in \mathbb{X}$, we will get

$$\phi(\mathbb{A}_1, \mathbb{A}_2) d(G(\mathbb{A}_1), G(\mathbb{A}_2)) \leq \psi(d(\mathbb{A}_1, \mathbb{A}_2)). \quad (28)$$

Thus, G is found as an ϕ - ψ -contraction. To verify that G is ϕ -admissible, let $\mathbb{A}_1, \mathbb{A}_2 \in \mathbb{X}$ be arbitrary and $\phi(\mathbb{A}_1, \mathbb{A}_2) \geq 1$. By definition of ϕ , we have

$$h(\mathbb{A}_1(\mathbf{t}), \mathbb{A}_2(\mathbf{t})) \geq 0. \quad (29)$$

Then, by (\wp_2), $h(G(\mathbb{A}_1(\mathbf{t})), G(\mathbb{A}_2(\mathbf{t}))) \geq 0$ is satisfied. Again, the definition of ϕ gives $\phi(G(\mathbb{A}_1), G(\mathbb{A}_2)) \geq 1$. Thus, G is ϕ -admissible.

On the other hand, the condition (\wp_2) guarantees the existence of $\mathbb{A}_0 \in \mathbb{X}$. In this case, for each $\mathbf{t} \in \mathbb{I}$, $h(\mathbb{A}_0(\mathbf{t}), G(\mathbb{A}_0(\mathbf{t}))) \geq 0$ holds. Clearly, we get $\phi(\mathbb{A}_0, G(\mathbb{A}_0)) \geq 1$. These show that the conditions (1) and (2) of Theorem 4 are fulfilled.

Now, we assume that $\{\mathbb{A}_n\}_{n \geq 1} \subseteq \mathbb{X}$ such that $\mathbb{A}_n \longrightarrow \mathbb{A}$ and for all n , $\phi(\mathbb{A}_n, \mathbb{A}_{n+1}) \geq 1$. By virtue of the definition of the nonnegative function ϕ ,

$$h(\mathbb{A}_n(\mathbf{t}), \mathbb{A}_{n+1}(\mathbf{t})) \geq 0. \quad (30)$$

Therefore, in the light of hypothesis (\wp_3), we obtain

$$h(\mathbb{A}_n(\mathbf{t}), \mathbb{A}(\mathbf{t})) \geq 0. \quad (31)$$

This indicates that $\phi(\mathbb{A}_n, \mathbb{A}) \geq 1$ for every n . This guarantees the condition (3) of Theorem 4. Ultimately, by using Theorem 4, we conclude that there is a fixed point for G like $\mathbb{A}^* \in \mathbb{X}$. This implies that $\mathbb{A}^* = (\mathcal{P}^*, \mathcal{S}^*, \mathcal{Q}^*)^T$ is interpreted as a solution of the fractal-fractional model of second-hand smoker (7), and the proof is completed. \square

In the sequel, we use the Leray-Schauder fixed point theorem to prove the existence result.

Theorem 6 (see [41]). Let \mathbb{X} be a Banach space, \mathbb{E} a bounded convex closed set in \mathbb{X} , and $\mathbb{O} \subset \mathbb{E}$ an open set with $0 \in \mathbb{O}$. Then, for the continuous and compact mapping $G : \mathbb{O} \longrightarrow \mathbb{E}$, either

(P1) There is $u \in \mathbb{O}$ such that $u = G(u)$ or

(P2) There is $u \in \partial \mathbb{O}$ and $0 < \mu < 1$ such that $u = \mu G(u)$.

Theorem 7. Suppose that $\mathbb{W} \in C(\mathbb{I} \times \mathbb{X}, \mathbb{X})$ and

(C1) There are $\varphi \in L^1(\mathbb{I}, \mathbb{R}^+)$ and increasing function $A \in C([0, \infty), (0, \infty))$ such that for each $\mathbf{t} \in \mathbb{I}$ and $\mathbb{A} \in \mathbb{X}$,

$$|\mathbb{W}(\mathbf{t}, \mathbb{A}(\mathbf{t}))| \leq \varphi(\mathbf{t})A(|\mathbb{A}(\mathbf{t})|). \quad (32)$$

(C2) There is $\alpha > 0$ such that

$$\frac{\alpha}{\mathbb{A}_0 + (\nu T^{\nu+\omega-1} \Gamma(\nu)/\Gamma(\nu+\omega)) \varphi_0^* A(\alpha)} > 1, \quad (33)$$

where $\varphi_0^* = \sup_{\mathbf{t} \in \mathbb{I}} |\varphi(\mathbf{t})|$.

Then, there is a solution for the fractal-fractional problem (13), and so there is a solution for the given fractal-fractional model of second-hand smokers (7) on \mathbb{I} .

Proof. To begin the proof, consider $G : \mathbb{X} \rightarrow \mathbb{X}$ formulated by (17) and the ball

$$N_\varepsilon = \{\mathbb{A} \in \mathbb{X} : \|\mathbb{A}\|_\mathbb{X} \leq \varepsilon\}, \quad (34)$$

for some $\varepsilon > 0$. In the first place, the continuity of \mathbb{W} yields that of the operator G . Now, by (C1), we have

$$\begin{aligned} |G(\mathbb{A}(\mathbf{t}))| &\leq |\mathbb{A}(0)| + \frac{\nu}{\Gamma(\omega)} \int_0^{\mathbf{t}} \mathbf{w}^{\nu-1} (\mathbf{t} - \mathbf{w})^{\omega-1} |\mathbb{W}(\mathbf{w}, \mathbb{A}(\mathbf{w}))| d\mathbf{w} \\ &\leq \mathbb{A}_0 + \frac{\nu}{\Gamma(\omega)} \int_0^{\mathbf{t}} \mathbf{w}^{\nu-1} (\mathbf{t} - \mathbf{w})^{\omega-1} \varphi(\mathbf{w}) A(|\mathbb{A}(\mathbf{w})|) d\mathbf{w} \\ &\leq \mathbb{A}_0 + \frac{\nu T^{\nu+\omega-1} \mathbb{B}(\nu, \omega)}{\Gamma(\omega)} \varphi_0^* A(\|\mathbb{A}\|_\mathbb{X}) \\ &\leq \mathbb{A}_0 + \frac{\nu T^{\nu+\omega-1} \Gamma(\nu)}{\Gamma(\nu+\omega)} \varphi_0^* A(\varepsilon), \end{aligned} \quad (35)$$

for each $\mathbb{A} \in N_\varepsilon$. In consequence, we obtain

$$\|G\mathbb{A}\|_\mathbb{X} \leq \mathbb{A}_0 + \frac{\nu T^{\nu+\omega-1} \Gamma(\nu)}{\Gamma(\nu+\omega)} \varphi_0^* A(\varepsilon) < \infty. \quad (36)$$

Hence, G is uniformly bounded on \mathbb{X} . In the sequel, the equicontinuity of G is investigated. To prove such a claim, for every $\mathbf{t}, \mathbf{t}_* \in [0, T]$ such that $\mathbf{t} < \mathbf{t}_*$ and for each $\mathbb{A} \in N_\varepsilon$, by letting

$$\sup_{(\mathbf{t}, \mathbb{A}) \in \mathbb{I} \times N_\varepsilon} |\mathbb{W}(\mathbf{t}, \mathbb{A}(\mathbf{t}))| = \mathbb{W}^* < \infty, \quad (37)$$

we have

$$\begin{aligned} &|G(\mathbb{A}(\mathbf{t}_*)) - G(\mathbb{A}(\mathbf{t}))| \\ &\leq \left| \frac{\nu}{\Gamma(\omega)} \int_0^{\mathbf{t}_*} \mathbf{w}^{\nu-1} (\mathbf{t}_* - \mathbf{w})^{\omega-1} \mathbb{W}(\mathbf{w}, \mathbb{A}(\mathbf{w})) d\mathbf{w} \right. \\ &\quad \left. - \frac{\nu}{\Gamma(\omega)} \int_0^{\mathbf{t}} \mathbf{w}^{\nu-1} (\mathbf{t} - \mathbf{w})^{\omega-1} \mathbb{W}(\mathbf{w}, \mathbb{A}(\mathbf{w})) d\mathbf{w} \right| \\ &\leq \frac{\nu \mathbb{W}^*}{\Gamma(\omega)} \left| \int_0^{\mathbf{t}_*} \mathbf{w}^{\nu-1} (\mathbf{t}_* - \mathbf{w})^{\omega-1} d\mathbf{w} - \int_0^{\mathbf{t}} \mathbf{w}^{\nu-1} (\mathbf{t} - \mathbf{w})^{\omega-1} d\mathbf{w} \right| \\ &\leq \frac{\nu \mathbb{W}^* \mathbb{B}(\nu, \omega)}{\Gamma(\omega)} [\mathbf{t}_*^{\nu+\omega-1} - \mathbf{t}^{\nu+\omega-1}] \\ &= \frac{\nu \mathbb{W}^* \Gamma(\nu)}{\Gamma(\nu+\omega)} [\mathbf{t}_*^{\nu+\omega-1} - \mathbf{t}^{\nu+\omega-1}], \end{aligned} \quad (38)$$

which is independent of \mathbb{A} , and the right-hand side of (38) converges to 0 as $\mathbf{t}_* \rightarrow \mathbf{t}$. Therefore, this implies that

$$\|G(\mathbb{A}(\mathbf{t}_*)) - G(\mathbb{A}(\mathbf{t}))\|_\mathbb{X} \rightarrow 0, \quad (39)$$

as $\mathbf{t}_* \rightarrow \mathbf{t}$. Thus, G is equicontinuous and is compact on N_ε by referring to the Arzelà–Ascoli theorem. We found that the conditions of Theorem 6 are valid on G . So, one of (P1) or (P2) will be fulfilled. By (C2), set

$$\mathbb{O} := \{\mathbb{A} \in \mathbb{X} : \|\mathbb{A}\|_\mathbb{X} < \alpha\}, \quad (40)$$

for some $\alpha > 0$ via $\mathbb{A}_0 + (\nu T^{\nu+\omega-1} \Gamma(\nu)/\Gamma(\nu+\omega)) \varphi_0^* A(\alpha) < \alpha$. With the help of (C1) and by (36), we write

$$\|G\mathbb{A}\|_\mathbb{X} \leq \mathbb{A}_0 + \frac{\nu T^{\nu+\omega-1} \Gamma(\nu)}{\Gamma(\nu+\omega)} \varphi_0^* A(\mathbb{A}). \quad (41)$$

Now, we assume the existence of $\mathbb{A} \in \partial \mathbb{O}$ and $0 < \mu < 1$ with $\mathbb{A} = \mu G(\mathbb{A})$. For these selections of \mathbb{A} and μ , and by (41), one may write

$$\begin{aligned} \alpha &= \|\mathbb{A}\|_\mathbb{X} = \mu \|G\mathbb{A}\|_\mathbb{X} < \mathbb{A}_0 + \frac{\nu T^{\nu+\omega-1} \Gamma(\nu)}{\Gamma(\nu+\omega)} \varphi_0^* A(\|\mathbb{A}\|_\mathbb{X}) \\ &< \mathbb{A}_0 + \frac{\nu T^{\nu+\omega-1} \Gamma(\nu)}{\Gamma(\nu+\omega)} \varphi_0^* A(\alpha) < \alpha, \end{aligned} \quad (42)$$

and this cannot occur. Therefore, the case (P2) does not hold and G has a fixed-point in $\bar{\mathbb{O}}$ by Theorem 6 which is interpreted as a solution of the fractal-fractional model of second-hand smoker (SHS) (7), and the proof is completed. \square

5. Uniqueness result

To prove the uniqueness of solution of the given fractal-fractional model of second-hand smoker (7), we use the Lipschitz property of functions \mathbb{W}_i , ($i = 1, 2, 3$) given by (11).

Lemma 8. Consider the functions $\mathcal{P}, \mathcal{S}, \mathcal{Q}, \mathcal{P}^*, \mathcal{S}^*, \mathcal{Q}^* \in \mathbb{M} := C(\mathbb{I}, \mathbb{R})$. Let

(H1) $\|\mathcal{P}\| \leq \lambda_1$, $\|\mathcal{S}\| \leq \lambda_2$, and $\|\mathcal{Q}\| \leq \lambda_3$ for some constants $\lambda_1, \lambda_2, \lambda_3 > 0$.

Then, the functions $\mathbb{W}_1, \mathbb{W}_2, \mathbb{W}_3$ introduced by (11) are satisfied the Lipschitz property with respect to the corresponding components if $w_1, w_2, w_3 > 0$, where

$$\begin{aligned} w_1 &= s + q_1 + r + b\lambda_2, w_2 \\ &= b\lambda_1 + r_1\lambda_3 + q_1 + q_2 + r_2, w_3 \\ &= r_1\lambda_2 + q_3 + q_1 + \gamma. \end{aligned} \quad (43)$$

Proof. We begin with the function \mathbb{W}_1 . For each $\mathcal{P}, \mathcal{P}^* \in \mathbb{M} := C(\mathbb{I}, \mathbb{R})$, we have

$$\begin{aligned} &\|\mathbb{W}_1(\mathbf{t}, \mathcal{P}(\mathbf{t}), \mathcal{S}(\mathbf{t}), \mathcal{Q}(\mathbf{t})) - \mathbb{W}_1(\mathbf{t}, \mathcal{P}^*(\mathbf{t}), \mathcal{S}(\mathbf{t}), \mathcal{Q}(\mathbf{t}))\| \\ &= \|(\theta - (s + q_1 + r)\mathcal{P}(\mathbf{t}) - b\mathcal{S}(\mathbf{t})\mathcal{P}(\mathbf{t})) \\ &\quad - (\theta - (s + q_1 + r)\mathcal{P}^*(\mathbf{t}) - b\mathcal{S}(\mathbf{t})\mathcal{P}^*(\mathbf{t}))\| \\ &\leq [(q_1 + s + r) + b\|\mathcal{S}(\mathbf{t})\|]\|\mathcal{P}(\mathbf{t}) - \mathcal{P}^*(\mathbf{t})\| \\ &\leq [(q_1 + s + r) + b\lambda_2]\|\mathcal{P}(\mathbf{t}) - \mathcal{P}^*(\mathbf{t})\| \\ &= w_1\|\mathcal{P}(\mathbf{t}) - \mathcal{P}^*(\mathbf{t})\|. \end{aligned} \quad (44)$$

This shows that \mathbb{W}_1 is Lipschitz with respect to \mathcal{P} with the Lipschitz constant $w_1 > 0$. For the function \mathbb{W}_2 , for each $\mathcal{S}, \mathcal{S}^* \in \mathbb{M} := C(\mathbb{I}, \mathbb{R})$, we have

$$\begin{aligned} &\|\mathbb{W}_2(\mathbf{t}, \mathcal{P}(\mathbf{t}), \mathcal{S}(\mathbf{t}), \mathcal{Q}(\mathbf{t})) - \mathbb{W}_2(\mathbf{t}, \mathcal{P}(\mathbf{t}), \mathcal{S}^*(\mathbf{t}), \mathcal{Q}(\mathbf{t}))\| \\ &= \|(b\mathcal{P}(\mathbf{t})\mathcal{S}(\mathbf{t}) + r_1\mathcal{Q}(\mathbf{t})\mathcal{S}(\mathbf{t}) - (q_1 + r_2 + q_2)\mathcal{S}(\mathbf{t})) \\ &\quad - (b\mathcal{P}(\mathbf{t})\mathcal{S}^*(\mathbf{t}) + r_1\mathcal{Q}(\mathbf{t})\mathcal{S}^*(\mathbf{t}) - (q_1 + r_2 + q_2)\mathcal{S}^*(\mathbf{t}))\| \\ &\leq [b\|\mathcal{P}(\mathbf{t})\| + r_1\|\mathcal{Q}(\mathbf{t})\| + (q_1 + r_2 + q_2)]\|\mathcal{S}(\mathbf{t}) - \mathcal{S}^*(\mathbf{t})\| \\ &\leq [b\lambda_1 + r_1\lambda_3 + q_1 + r_2 + q_2]\|\mathcal{S}(\mathbf{t}) - \mathcal{S}^*(\mathbf{t})\| \\ &= w_2\|\mathcal{S}(\mathbf{t}) - \mathcal{S}^*(\mathbf{t})\|. \end{aligned} \quad (45)$$

This shows that \mathbb{W}_2 is Lipschitz with respect to \mathcal{S} with the Lipschitz constant $w_2 > 0$. Now, for each $\mathcal{Q}, \mathcal{Q}^* \in \mathbb{M} := C(\mathbb{I}, \mathbb{R})$, we have

$$\begin{aligned} &\|\mathbb{W}_3(\mathbf{t}, \mathcal{P}(\mathbf{t}), \mathcal{S}(\mathbf{t}), \mathcal{Q}(\mathbf{t})) - \mathbb{W}_3(\mathbf{t}, \mathcal{P}(\mathbf{t}), \mathcal{S}(\mathbf{t}), \mathcal{Q}^*(\mathbf{t}))\| \\ &= \|(r_2\mathcal{S}(\mathbf{t}) - r_1\mathcal{S}(\mathbf{t})\mathcal{Q}(\mathbf{t}) - (q_3 + q_1 + \gamma)\mathcal{Q}(\mathbf{t})) \\ &\quad - (r_2\mathcal{S}(\mathbf{t}) - r_1\mathcal{S}(\mathbf{t})\mathcal{Q}^*(\mathbf{t}) - (q_3 + q_1 + \gamma)\mathcal{Q}^*(\mathbf{t}))\| \\ &\leq [r_1\|\mathcal{S}(\mathbf{t})\| + q_3 + q_1 + \gamma]\|\mathcal{Q}(\mathbf{t}) - \mathcal{Q}^*(\mathbf{t})\| \\ &\leq [r_1\lambda_2 + q_3 + q_1 + \gamma]\|\mathcal{Q}(\mathbf{t}) - \mathcal{Q}^*(\mathbf{t})\| \\ &= w_3\|\mathcal{Q}(\mathbf{t}) - \mathcal{Q}^*(\mathbf{t})\|. \end{aligned} \quad (46)$$

Accordingly, this shows that \mathbb{W}_3 is Lipschitz with respect to \mathcal{Q} with the Lipschitz constant $w_3 > 0$. Above results show that three functions $\mathbb{W}_1, \mathbb{W}_2, \mathbb{W}_3$ are Lipschitzian with respect to the corresponding component with the Lipschitz constants $w_1, w_2, w_3 > 0$, respectively. \square

According to the obtained results in Lemma 8, we investigate the uniqueness property for solution to the supposed fractal-fractional system (7).

Theorem 9. Let (H1) holds. Then, the given fractal-fractional model of second-hand smoker (7) has a unique solution if

$$\frac{\nu T^{\nu+\omega-1}\Gamma(\nu)}{\Gamma(\nu+\omega)} w_i < 1, i \in \{1, 2, 3\}. \quad (47)$$

Proof. We assume that the conclusion of theorem is not valid. In other words, there is another solution for the given fractal-fractional model of second-hand smoker (7). Assume that $(\mathcal{P}^*(\mathbf{t}), \mathcal{S}^*(\mathbf{t}), \mathcal{Q}^*(\mathbf{t}))$ is another solution with initial conditions $(\mathcal{P}_0, \mathcal{S}_0, \mathcal{Q}_0)$ such that by (16), we have

$$\begin{aligned} \mathcal{P}^*(\mathbf{t}) &= \mathcal{P}_0 + \frac{\nu}{\Gamma(\omega)} \int_0^t \mathbf{w}^{\nu-1}(\mathbf{t} - \mathbf{w})^{\omega-1} \mathbb{W}_1(\mathbf{w}, \mathcal{P}^*(\mathbf{w}), \mathcal{S}^*(\mathbf{w}), \mathcal{Q}^*(\mathbf{w})) d\mathbf{w}, \\ \mathcal{S}^*(\mathbf{t}) &= \mathcal{S}_0 + \frac{\nu}{\Gamma(\omega)} \int_0^t \mathbf{w}^{\nu-1}(\mathbf{t} - \mathbf{w})^{\omega-1} \mathbb{W}_2(\mathbf{w}, \mathcal{P}^*(\mathbf{w}), \mathcal{S}^*(\mathbf{w}), \mathcal{Q}^*(\mathbf{w})) d\mathbf{w}, \\ \mathcal{Q}^*(\mathbf{t}) &= \mathcal{Q}_0 + \frac{\nu}{\Gamma(\omega)} \int_0^t \mathbf{w}^{\nu-1}(\mathbf{t} - \mathbf{w})^{\omega-1} \mathbb{W}_3(\mathbf{w}, \mathcal{P}^*(\mathbf{w}), \mathcal{S}^*(\mathbf{w}), \mathcal{Q}^*(\mathbf{w})) d\mathbf{w}. \end{aligned} \quad (48)$$

Now, we can estimate

$$\begin{aligned} |\mathcal{P}(\mathbf{t}) - \mathcal{P}^*(\mathbf{t})| &\leq \frac{\nu}{\Gamma(\omega)} \int_0^t \mathbf{w}^{\nu-1}(\mathbf{t} - \mathbf{w})^{\omega-1} \\ &\quad \times |\mathbb{W}_1(\mathbf{w}, \mathcal{P}(\mathbf{w}), \mathcal{S}(\mathbf{w}), \mathcal{Q}(\mathbf{w})) \\ &\quad - \mathbb{W}_1(\mathbf{w}, \mathcal{P}^*(\mathbf{w}), \mathcal{S}^*(\mathbf{w}), \mathcal{Q}^*(\mathbf{w}))| d\mathbf{w} \\ &\leq \frac{\nu}{\Gamma(\omega)} \int_0^t \mathbf{w}^{\nu-1}(\mathbf{t} - \mathbf{w})^{\omega-1} w_1 \|\mathcal{P} - \mathcal{P}^*\| d\mathbf{w} \\ &\leq \frac{\nu T^{\nu+\omega-1}\Gamma(\nu)}{\Gamma(\nu+\omega)} w_1 \|\mathcal{P} - \mathcal{P}^*\|, \end{aligned} \quad (49)$$

and so

$$\left[1 - \frac{\nu T^{\nu+\omega-1}\Gamma(\nu)}{\Gamma(\nu+\omega)} w_1\right] \|\mathcal{P} - \mathcal{P}^*\| \leq 0. \quad (50)$$

The latter inequality is true if $\|\mathcal{P} - \mathcal{P}^*\| = 0$, and accordingly, $\mathcal{P} = \mathcal{P}^*$. Similarly, from

$$\|\mathcal{S} - \mathcal{S}^*\| \leq \frac{\nu T^{\nu+\omega-1}\Gamma(\nu)}{\Gamma(\nu+\omega)} w_2 \|\mathcal{S} - \mathcal{S}^*\|, \quad (51)$$

we get

$$\left[1 - \frac{\nu T^{\nu+\omega-1}\Gamma(\nu)}{\Gamma(\nu+\omega)} w_2\right] \|\mathcal{S} - \mathcal{S}^*\| \leq 0. \quad (52)$$

This implies that $\|\mathcal{S} - \mathcal{S}^*\| = 0$ and so $\mathcal{S} = \mathcal{S}^*$. Also,

$$\|\mathcal{Q} - \mathcal{Q}^*\| \leq \frac{\nu T^{\nu+\omega-1} \Gamma(\nu)}{\Gamma(\nu+\omega)} w_3 \|\mathcal{Q} - \mathcal{Q}^*\|. \quad (53)$$

This gives

$$\left[1 - \frac{\nu T^{\nu+\omega-1} \Gamma(\nu)}{\Gamma(\nu+\omega)} w_3 \right] \|\mathcal{Q} - \mathcal{Q}^*\| \leq 0. \quad (54)$$

Hence, $\mathcal{Q} = \mathcal{Q}^*$. Consequently, we get

$$(\mathcal{P}(\mathbf{t}), \mathcal{S}(\mathbf{t}), \mathcal{Q}(\mathbf{t})) = (\mathcal{P}^*(\mathbf{t}), \mathcal{S}^*(\mathbf{t}), \mathcal{Q}^*(\mathbf{t})). \quad (55)$$

This shows that the fractal-fractional model of second-hand smoker (7) has a unique solution, and this completes our proof. \square

6. Stability

Here, the stability notion in the sense of the Ulam–Hyers, Ulam–Hyers–Rassias, and their generalized versions is established for the system of fractal-fractional SHS-model (7). For more details on the stability analysis, we refer to [46, 47].

Definition 10. The fractal-fractional model of SHS (7) is Ulam–Hyers stable if there are $0 < M_{\mathbb{W}_i} \in \mathbb{R}$, ($i \in \{1, 2, 3\}$) such that for each $\varepsilon_i > 0$, and for each $(\mathcal{P}^*, \mathcal{S}^*, \mathcal{Q}^*) \in \mathbb{X}$ satisfying

$$\begin{cases} |{}^{FFP}\mathfrak{D}_{0,t}^{\omega,\nu} \mathcal{P}^*(\mathbf{t}) - \mathbb{W}_1(\mathbf{t}, \mathcal{P}^*(\mathbf{t}), \mathcal{S}^*(\mathbf{t}), \mathcal{Q}^*(\mathbf{t}))| < \varepsilon_1, \\ |{}^{FFP}\mathfrak{D}_{0,t}^{\omega,\nu} \mathcal{S}^*(\mathbf{t}) - \mathbb{W}_2(\mathbf{t}, \mathcal{P}^*(\mathbf{t}), \mathcal{S}^*(\mathbf{t}), \mathcal{Q}^*(\mathbf{t}))| < \varepsilon_2, \\ |{}^{FFP}\mathfrak{D}_{0,t}^{\omega,\nu} \mathcal{Q}^*(\mathbf{t}) - \mathbb{W}_3(\mathbf{t}, \mathcal{P}^*(\mathbf{t}), \mathcal{S}^*(\mathbf{t}), \mathcal{Q}^*(\mathbf{t}))| < \varepsilon_3, \end{cases} \quad (56)$$

there is $(\mathcal{P}, \mathcal{S}, \mathcal{Q}) \in \mathbb{X}$ satisfying the given fractal-fractional model (7) such that

$$\begin{cases} |\mathcal{P}^*(\mathbf{t}) - \mathcal{P}(\mathbf{t})| \leq M_{\mathbb{W}_1} \varepsilon_1, \\ |\mathcal{S}^*(\mathbf{t}) - \mathcal{S}(\mathbf{t})| \leq M_{\mathbb{W}_2} \varepsilon_2, \\ |\mathcal{Q}^*(\mathbf{t}) - \mathcal{Q}(\mathbf{t})| \leq M_{\mathbb{W}_3} \varepsilon_3. \end{cases} \quad (57)$$

Definition 11. The given fractal-fractional model of second-hand smoker (7) is generalized Ulam–Hyers stable if there are $M_{\mathbb{W}_i} \in C(\mathbb{R}^+, \mathbb{R}^+)$, ($i \in \{1, 2, 3\}$) with $M_{\mathbb{W}_i}(0) = 0$ such that for each $\varepsilon_i > 0$ and for each $(\mathcal{P}^*, \mathcal{S}^*, \mathcal{Q}^*) \in \mathbb{X}$ satisfying the inequalities (56), there is $(\mathcal{P}, \mathcal{S}, \mathcal{Q}) \in \mathbb{X}$ as a solution of the given fractal-fractional model of second-hand smoker (7) such that

$$\begin{cases} |\mathcal{P}^*(\mathbf{t}) - \mathcal{P}(\mathbf{t})| \leq M_{\mathbb{W}_1}(\varepsilon_1), \\ |\mathcal{S}^*(\mathbf{t}) - \mathcal{S}(\mathbf{t})| \leq M_{\mathbb{W}_2}(\varepsilon_2), \\ |\mathcal{Q}^*(\mathbf{t}) - \mathcal{Q}(\mathbf{t})| \leq M_{\mathbb{W}_3}(\varepsilon_3). \end{cases} \quad (58)$$

Note that Definition 11 is derived from Definition 10.

Remark 12. Notice that $(\mathcal{P}^*, \mathcal{S}^*, \mathcal{Q}^*) \in \mathbb{X}$ is a solution for (56) if and only if there are $\hbar_1, \hbar_2, \hbar_3 \in C([0, T], \mathbb{R})$ (depending on $\mathcal{P}^*, \mathcal{S}^*, \mathcal{Q}^*$, respectively) such that for each $\mathbf{t} \in \mathbb{I}$,

$$|\hbar_i(\mathbf{t})| < \varepsilon_i. \quad (59)$$

(1) We have

$$\begin{cases} {}^{FFP}\mathfrak{D}_{0,t}^{\omega,\nu} \mathcal{P}^*(\mathbf{t}) - \mathbb{W}_1(\mathbf{t}, \mathcal{P}^*(\mathbf{t}), \mathcal{S}^*(\mathbf{t}), \mathcal{Q}^*(\mathbf{t})) + \hbar_1(\mathbf{t}), \\ {}^{FFP}\mathfrak{D}_{0,t}^{\omega,\nu} \mathcal{S}^*(\mathbf{t}) - \mathbb{W}_2(\mathbf{t}, \mathcal{P}^*(\mathbf{t}), \mathcal{S}^*(\mathbf{t}), \mathcal{Q}^*(\mathbf{t})) + \hbar_2(\mathbf{t}), \\ {}^{FFP}\mathfrak{D}_{0,t}^{\omega,\nu} \mathcal{Q}^*(\mathbf{t}) - \mathbb{W}_3(\mathbf{t}, \mathcal{P}^*(\mathbf{t}), \mathcal{S}^*(\mathbf{t}), \mathcal{Q}^*(\mathbf{t})) + \hbar_3(\mathbf{t}), \end{cases} \quad (60)$$

Definition 13. The given fractal-fractional model of second-hand smoker (7) is Ulam–Hyers–Rassias stable with respect to functions Φ_i , ($i \in \{1, 2, 3\}$) if there are $0 < M_{(\mathbb{W}_i, \Phi_i)} \in \mathbb{R}$ such that for each $\varepsilon_i > 0$ and for each $(\mathcal{P}^*, \mathcal{S}^*, \mathcal{Q}^*) \in \mathbb{X}$ satisfying

$$\begin{cases} |{}^{FFP}\mathfrak{D}_{0,t}^{\omega,\nu} \mathcal{P}^*(\mathbf{t}) - \mathbb{W}_1(\mathbf{t}, \mathcal{P}^*(\mathbf{t}), \mathcal{S}^*(\mathbf{t}), \mathcal{Q}^*(\mathbf{t}))| < \varepsilon_1 \Phi_1(\mathbf{t}), \\ |{}^{FFP}\mathfrak{D}_{0,t}^{\omega,\nu} \mathcal{S}^*(\mathbf{t}) - \mathbb{W}_2(\mathbf{t}, \mathcal{P}^*(\mathbf{t}), \mathcal{S}^*(\mathbf{t}), \mathcal{Q}^*(\mathbf{t}))| < \varepsilon_2 \Phi_2(\mathbf{t}), \\ |{}^{FFP}\mathfrak{D}_{0,t}^{\omega,\nu} \mathcal{Q}^*(\mathbf{t}) - \mathbb{W}_3(\mathbf{t}, \mathcal{P}^*(\mathbf{t}), \mathcal{S}^*(\mathbf{t}), \mathcal{Q}^*(\mathbf{t}))| < \varepsilon_3 \Phi_3(\mathbf{t}), \end{cases} \quad (61)$$

there is $(\mathcal{P}, \mathcal{S}, \mathcal{Q}) \in \mathbb{X}$ as a solution of the given fractal-fractional model of second-hand smoker (7) such that

$$\begin{cases} |\mathcal{P}^*(\mathbf{t}) - \mathcal{P}(\mathbf{t})| \leq \varepsilon_1 M_{(\mathbb{W}_1, \Phi_1)} \Phi_1(\mathbf{t}), \forall \mathbf{t} \in \mathbb{I}, \\ |\mathcal{S}^*(\mathbf{t}) - \mathcal{S}(\mathbf{t})| \leq \varepsilon_2 M_{(\mathbb{W}_2, \Phi_2)} \Phi_2(\mathbf{t}), \forall \mathbf{t} \in \mathbb{I}, \\ |\mathcal{Q}^*(\mathbf{t}) - \mathcal{Q}(\mathbf{t})| \leq \varepsilon_3 M_{(\mathbb{W}_3, \Phi_3)} \Phi_3(\mathbf{t}), \forall \mathbf{t} \in \mathbb{I}. \end{cases} \quad (62)$$

Definition 14. The given fractal-fractional model of second-hand smoker (7) is generalized Ulam–Hyers–Rassias stable with respect to functions Φ_i if there are $0 < M_{(\mathbb{W}_i, \Phi_i)} \in \mathbb{R}$ such that for each $(\mathcal{P}^*, \mathcal{S}^*, \mathcal{Q}^*) \in \mathbb{X}$ satisfying

$$\begin{cases} \left| {}^{FFP}\mathfrak{D}_{0,t}^{\omega,\nu} \mathcal{P}^*(t) - \mathbb{W}_1(t, \mathcal{P}^*(t), \mathcal{S}^*(t), \mathcal{Q}^*(t)) \right| < \Phi_1(t), \\ \left| {}^{FFP}\mathfrak{D}_{0,t}^{\omega,\nu} \mathcal{S}^*(t) - \mathbb{W}_2(t, \mathcal{P}^*(t), \mathcal{S}^*(t), \mathcal{Q}^*(t)) \right| < \Phi_2(t), \\ \left| {}^{FFP}\mathfrak{D}_{0,t}^{\omega,\nu} \mathcal{Q}^*(t) - \mathbb{W}_3(t, \mathcal{P}^*(t), \mathcal{S}^*(t), \mathcal{Q}^*(t)) \right| < \Phi_3(t), \end{cases} \quad (63)$$

there is $(\mathcal{P}, \mathcal{S}, \mathcal{Q}) \in \mathbb{X}$ as a solution of the given fractal-fractional model of second-hand smoker (7) such that

$$\begin{cases} |\mathcal{P}^*(t) - \mathcal{P}(t)| \leq M_{(\mathbb{W}_1, \Phi_1)} \Phi_1(t), \\ |\mathcal{S}^*(t) - \mathcal{S}(t)| \leq M_{(\mathbb{W}_2, \Phi_2)} \Phi_2(t), \\ |\mathcal{Q}^*(t) - \mathcal{Q}(t)| \leq M_{(\mathbb{W}_3, \Phi_3)} \Phi_3(t). \end{cases} \quad (64)$$

Note that Definition 14 is derived from Definition 13. Also, if we take $\Phi_i(t) = 1$, then Definition 13 gives the Ulam-Hyers property for the stability of solutions.

Remark 16. Notice that $(\mathcal{P}^*, \mathcal{S}^*, \mathcal{Q}^*) \in \mathbb{X}$ is a solution for (61) if and only if there are $\hbar_1, \hbar_2, \hbar_3 \in C([0, T], \mathbb{R})$ (depending on $\mathcal{P}^*, \mathcal{S}^*, \mathcal{Q}^*$, respectively) such that $\forall t \in \mathbb{I}$,

$$|\hbar_i(t)| < \varepsilon_i \Phi_i(\mathfrak{T}). \quad (65)$$

(i) We have

$$\begin{cases} {}^{FFP}\mathfrak{D}_{0,t}^{\omega,\nu} \mathcal{P}^*(t) = \mathbb{W}_1(t, \mathcal{P}^*(t), \mathcal{S}^*(t), \mathcal{Q}^*(t)) + \hbar_1(t), \\ {}^{FFP}\mathfrak{D}_{0,t}^{\omega,\nu} \mathcal{S}^*(t) = \mathbb{W}_2(t, \mathcal{P}^*(t), \mathcal{S}^*(t), \mathcal{Q}^*(t)) + \hbar_2(t), \\ {}^{FFP}\mathfrak{D}_{0,t}^{\omega,\nu} \mathcal{Q}^*(t) = \mathbb{W}_3(t, \mathcal{P}^*(t), \mathcal{S}^*(t), \mathcal{Q}^*(t)) + \hbar_3(t). \end{cases} \quad (66)$$

The Ulam-Hyers stability is discussed here to the given fractal-fractional model of second-hand smoker (7).

Theorem 17. If the assumption (H1) is fulfilled, then the given fractal-fractional model of second-hand smoker (7) is Ulam-Hyers stable on $\mathbb{I} := [0, T]$ and also is generalized Ulam-Hyers stable such that

$$\frac{\nu T^{\nu+\omega-1} \Gamma(\nu)}{\Gamma(\nu+\omega)} w_i < 1, i \in \{1, 2, 3\}, \quad (67)$$

where w_i is given by (43).

Proof. Let $\varepsilon_1 > 0$ and $\mathcal{P}^* \in \mathbb{M}$ be arbitrary such that

$$\left| {}^{FFP}\mathfrak{D}_{0,t}^{\omega,\nu} \mathcal{P}^*(t) - \mathbb{W}_1(t, \mathcal{P}^*(t), \mathcal{S}^*(t), \mathcal{Q}^*(t)) \right| < \varepsilon_1. \quad (68)$$

Then, from Remark 1, we can find a function $\hbar_1(t)$ satisfying

$${}^{FFP}\mathfrak{D}_{0,t}^{\omega,\nu} \mathcal{P}^*(t) = \mathbb{W}_1(t, \mathcal{P}^*(t), \mathcal{S}^*(t), \mathcal{Q}^*(t)) + \hbar_1(t), \quad (69)$$

with $|\hbar_1(t)| \leq \varepsilon_1$. It follows that

$$\begin{aligned} \mathcal{P}^*(t) &= \mathcal{P}_0 + \frac{\nu}{\Gamma(\omega)} \int_0^t \mathfrak{w}^{\nu-1} (t - \mathfrak{w})^{\omega-1} \mathbb{W}_1(\mathfrak{w}, \mathcal{P}^*(\mathfrak{w}), \mathcal{S}^*(\mathfrak{w}), \mathcal{Q}^*(\mathfrak{w})) d\mathfrak{w} \\ &\quad + \frac{\nu}{\Gamma(\omega)} \int_0^t \mathfrak{w}^{\nu-1} (t - \mathfrak{w})^{\omega-1} \hbar_1(\mathfrak{w}) d\mathfrak{w}. \end{aligned} \quad (70)$$

By Theorem 9, let $\mathcal{P} \in \mathbb{M}$ be the unique solution of the given fractal-fractional model of second-hand smoker (7). Then, $\mathcal{P}(t)$ is defined as

$$\mathcal{P}(t) = \mathcal{P}_0 + \frac{\nu}{\Gamma(\omega)} \int_0^t \mathfrak{w}^{\nu-1} (t - \mathfrak{w})^{\omega-1} \mathbb{W}_1(\mathfrak{w}, \mathcal{P}(\mathfrak{w}), \mathcal{S}(\mathfrak{w}), \mathcal{Q}(\mathfrak{w})) d\mathfrak{w}. \quad (71)$$

Therefore,

$$\begin{aligned} |\mathcal{P}^*(t) - \mathcal{P}(t)| &\leq \frac{\nu}{\Gamma(\omega)} \int_0^t \mathfrak{w}^{\nu-1} (t - \mathfrak{w})^{\omega-1} |\hbar_1(\mathfrak{w})| d\mathfrak{w} \\ &\quad + \frac{\nu}{\Gamma(\omega)} \int_0^t \mathfrak{w}^{\nu-1} (t - \mathfrak{w})^{\omega-1} \\ &\quad \times |\mathbb{W}_1(\mathfrak{w}, \mathcal{P}^*(\mathfrak{w}), \mathcal{S}^*(\mathfrak{w}), \mathcal{Q}^*(\mathfrak{w})) \\ &\quad - \mathbb{W}_1(\mathfrak{w}, \mathcal{P}(\mathfrak{w}), \mathcal{S}(\mathfrak{w}), \mathcal{Q}(\mathfrak{w}))| d\mathfrak{w} \\ &\leq \frac{\nu T^{\nu+\omega-1} \Gamma(\nu)}{\Gamma(\nu+\omega)} \varepsilon_1 + \frac{\nu T^{\nu+\omega-1} \Gamma(\nu)}{\Gamma(\nu+\omega)} w_1 \|\mathcal{P}^* - \mathcal{P}\|. \end{aligned} \quad (72)$$

Hence, we get

$$\|\mathcal{P}^* - \mathcal{P}\| \leq \frac{(\nu T^{\nu+\omega-1} \Gamma(\nu) / \Gamma(\nu+\omega)) \varepsilon_1}{1 - (\nu T^{\nu+\omega-1} \Gamma(\nu) / \Gamma(\nu+\omega)) w_1}. \quad (73)$$

If we let $M_{\mathbb{W}_1} = (\nu T^{\nu+\omega-1} \Gamma(\nu) / \Gamma(\nu+\omega)) / (1 - (\nu T^{\nu+\omega-1} \Gamma(\nu) / \Gamma(\nu+\omega)) w_1)$, then $\|\mathcal{P}^* - \mathcal{P}\| \leq M_{\mathbb{W}_1} \varepsilon_1$. Similarly, we have

$$\|\mathcal{S}^* - \mathcal{S}\| \leq M_{\mathbb{W}_2} \varepsilon_2, \quad \|\mathcal{Q}^* - \mathcal{Q}\| \leq M_{\mathbb{W}_3} \varepsilon_3, \quad (74)$$

where

$$M_{\mathbb{W}_i} = \frac{\nu T^{\nu+\omega-1} \Gamma(\nu) / \Gamma(\nu+\omega)}{1 - (\nu T^{\nu+\omega-1} \Gamma(\nu) / \Gamma(\nu+\omega)) w_i}, \quad (i \in \{2, 3\}). \quad (75)$$

Hence, the Ulam–Hyers stability of the given SHS-model (7) is fulfilled. Next, by assuming

$$M_{\mathbb{W}_i}(\varepsilon_i) = \frac{(\nu T^{\nu+\omega-1} \Gamma(\nu)/\Gamma(\nu+\omega))\varepsilon_i}{1 - (\nu T^{\nu+\omega-1} \Gamma(\nu)/\Gamma(\nu+\omega))w_i}, (i \in \{2, 3\}), \quad (76)$$

with $M_{\mathbb{W}_i}(0) = 0$, clearly, the generalized Ulam–Hyers stability is proved. \square

Theorem 18. *The condition (H1) is assumed to be held, and (H') There are increasing functions $\Phi_i \in C([0, T], \mathbb{R}^+)$, ($i \in \{1, 2, 3\}$), and $\Lambda_{\Phi_i} > 0$ such that*

$${}^{FFP}\mathfrak{D}_{0,t}^{\omega,\nu} \Phi_i(t) < \Lambda_{\Phi_i} \Phi_i(t), (i \in \{1, 2, 3\}), \forall t \in \mathbb{I}. \quad (77)$$

Then, the given fractal-fractional model of second-hand smoker (7) is the Ulam–Hyers–Rassias and generalized Ulam–Hyers–Rassias stable.

Proof. For each $\varepsilon_1 > 0$ and for each $\mathcal{P}^* \in \mathbb{M}$ satisfying

$$\left| {}^{FFP}\mathfrak{D}_{0,t}^{\omega,\nu} \mathcal{P}^*(t) - \mathbb{W}_1(t, \mathcal{P}^*(t), \mathcal{S}^*(t), \mathcal{Q}^*(t)) \right| < \varepsilon_1 \Phi_1(t), \quad (78)$$

we can find a function $\hbar_1(t)$ satisfying

$${}^{FFP}\mathfrak{D}_{0,t}^{\omega,\nu} \mathcal{P}^*(t) = \mathbb{W}_1(t, \mathcal{P}^*(t), \mathcal{S}^*(t), \mathcal{Q}^*(t)) + \hbar_1(t), \quad (79)$$

with $|\hbar_1(t)| \leq \varepsilon_1 \Phi_1(t)$. It gives

$$\begin{aligned} \mathcal{P}^*(t) &= \mathcal{P}_0 + \frac{\nu}{\Gamma(\omega)} \int_0^t \mathfrak{w}^{\nu-1} (t - \mathfrak{w})^{\omega-1} \mathbb{W}_1(\mathfrak{w}, \mathcal{P}^*(\mathfrak{w}), \mathcal{S}^*(\mathfrak{w}), \mathcal{Q}^*(\mathfrak{w})) d\mathfrak{w} \\ &\quad + \frac{\nu}{\Gamma(\omega)} \int_0^t \mathfrak{w}^{\nu-1} (t - \mathfrak{w})^{\omega-1} \hbar_1(\mathfrak{w}) d\mathfrak{w}. \end{aligned} \quad (80)$$

By Theorem 9, let $\mathcal{P} \in \mathbb{M}$ be the unique solution of the given fractal-fractional model of second-hand smoker (7). Then, $\mathcal{P}(t)$ is given by

$$\mathcal{P}(t) = \mathcal{P}_0 + \frac{\nu}{\Gamma(\omega)} \int_0^t \mathfrak{w}^{\nu-1} (t - \mathfrak{w})^{\omega-1} \mathbb{W}_1(\mathfrak{w}, \mathcal{P}(\mathfrak{w}), \mathcal{S}(\mathfrak{w}), \mathcal{Q}(\mathfrak{w})) d\mathfrak{w}. \quad (81)$$

Then, by (77),

$$\begin{aligned} |\mathcal{P}^*(t) - \mathcal{P}(t)| &\leq \frac{\nu}{\Gamma(\omega)} \int_0^t \mathfrak{w}^{\nu-1} (t - \mathfrak{w})^{\omega-1} |\hbar_1(\mathfrak{w})| d\mathfrak{w} \\ &\quad + \frac{\nu}{\Gamma(\omega)} \int_0^t \mathfrak{w}^{\nu-1} (t - \mathfrak{w})^{\omega-1} \\ &\quad \times |\mathbb{W}_1(\mathfrak{w}, \mathcal{P}^*(\mathfrak{w}), \mathcal{S}^*(\mathfrak{w}), \mathcal{Q}^*(\mathfrak{w})) \\ &\quad - \mathbb{W}_1(\mathfrak{w}, \mathcal{P}(\mathfrak{w}), \mathcal{S}(\mathfrak{w}), \mathcal{Q}(\mathfrak{w}))| d\mathfrak{w} \\ &\leq \frac{\varepsilon_1 \nu}{\Gamma(\omega)} \int_0^t \mathfrak{w}^{\nu-1} (t - \mathfrak{w})^{\omega-1} \Phi_1(\mathfrak{w}) d\mathfrak{w} \\ &\quad + \frac{\nu T^{\nu+\omega-1} \Gamma(\nu)}{\Gamma(\nu+\omega)} w_1 \|\mathcal{P}^* - \mathcal{P}\| \\ &\leq \varepsilon_1 \Lambda_{\Phi_1} \Phi_1(t) + \frac{\nu T^{\nu+\omega-1} \Gamma(\nu)}{\Gamma(\nu+\omega)} w_1 \|\mathcal{P}^* - \mathcal{P}\|. \end{aligned} \quad (82)$$

Accordingly, it gives

$$\|\mathcal{P}^* - \mathcal{P}\| \leq \frac{\varepsilon_1 \Lambda_{\Phi_1} \Phi_1(t)}{1 - (\nu T^{\nu+\omega-1} \Gamma(\nu)/\Gamma(\nu+\omega))w_1}. \quad (83)$$

If we let

$$M_{(\mathbb{W}_1, \Phi_1)} = \frac{\Lambda_{\Phi_1}}{1 - (\nu T^{\nu+\omega-1} \Gamma(\nu)/\Gamma(\nu+\omega))w_1}, \quad (84)$$

then $\|\mathcal{P}^* - \mathcal{P}\| \leq \varepsilon_1 M_{(\mathbb{W}_1, \Phi_1)} \Phi_1(t)$. Similarly, we have

$$\|\mathcal{S}^* - \mathcal{S}\| \leq \varepsilon_2 M_{(\mathbb{W}_2, \Phi_2)} \Phi_2(t), \|\mathcal{Q}^* - \mathcal{Q}\| \leq \varepsilon_3 M_{(\mathbb{W}_3, \Phi_3)} \Phi_3(t), \quad (85)$$

where

$$M_{(\mathbb{W}_i, \Phi_i)} = \frac{\Lambda_{\Phi_i}}{1 - (\nu T^{\nu+\omega-1} \Gamma(\nu)/\Gamma(\nu+\omega))w_i}, (i \in \{2, 3\}). \quad (86)$$

Hence, the given fractal-fractional model of second-hand smoker (7) is stable in the sense of Ulam–Hyers–Rassias. Along with this, by setting $\varepsilon_i = 1$, ($i \in \{1, 2, 3\}$), the mentioned fractal-fractional model of second-hand smoker (7) is generalized Ulam–Hyers–Rassias stable. \square

7. Steady-State Analysis and Local Stability

Here, we follow our investigation for obtaining equilibrium points of the supposed fractal-fractional system (7).

7.1. Disease-free equilibrium point. Define the following homogeneous system of equations:

$${}^{FFP}\mathfrak{D}_{0,t}^{\omega,\nu} \mathcal{P}(t) = {}^{FFP}\mathfrak{D}_{0,t}^{\omega,\nu} \mathcal{S}(t) = {}^{FFP}\mathfrak{D}_{0,t}^{\omega,\nu} \mathcal{Q}(t) = 0, \quad (87)$$

or equivalently

$$\begin{cases} \theta - (s + q_1 + r)\mathcal{P}(t) - b\mathcal{S}(t)\mathcal{P}(t) = 0, \\ b\mathcal{P}(t)\mathcal{S}(t) + r_1\mathcal{Q}(t)\mathcal{S}(t) - (q_1 + q_2 + r_2)\mathcal{S}(t) = 0, \\ r_2\mathcal{S}(t) - r_1\mathcal{S}(t)\mathcal{Q}(t) - (q_3 + q_1 + \gamma)\mathcal{Q}(t) = 0. \end{cases} \quad (88)$$

In this case, the (disease) smoke-free equilibrium point E^0 of the model of second-hand smoker (7) under no infection when $\mathcal{S}^0 = 0$ and $\mathcal{Q}^0 = 0$ is presented by

$$E^0 = \left(\frac{\theta}{s + q_1 + r}, 0, 0 \right). \quad (89)$$

7.2. Basic Reproduction Number. Here, we calculate the basic reproduction number with the help of the next generation matrix approach [48]. As we know, this quantity denoted by R_0 is considered as the expected value of the rate of infection in each time unit. The infection happens in the susceptible individuals due to the infected individuals, and also, the existence of the endemic equilibrium point to the fractal-fractional second-hand smoker model (7) depends on the value of R_0 . To do this, we consider the infected compartments $\mathcal{S}(t)$ and $\mathcal{Q}(t)$. By assuming $\mathcal{Y} = (\mathcal{S}, \mathcal{Q})^T$ and from the infected compartments, we have two vectors say f and v in which we have nonlinear terms in f and the negative of linear terms in v , satisfying

$$\frac{d\mathcal{Y}}{dt} \Big|_{E^0} = f - v, \quad (90)$$

where

$$f = \begin{bmatrix} b\mathcal{S}\mathcal{P} \\ 0 \\ 0 \end{bmatrix}, v = \begin{bmatrix} (q_1 + q_2 + r_2)\mathcal{S} \\ -\theta + (s + q_1 + r)\mathcal{P} + b\mathcal{S}\mathcal{P} \\ -r_2\mathcal{S} + r_1\mathcal{S}\mathcal{Q} + (q_3 + q_1 + \gamma)\mathcal{Q} \end{bmatrix}. \quad (91)$$

The Jacobian matrices of both matrices f and v are given by

$$\begin{aligned} \mathbb{J}[f] &= \begin{bmatrix} b\mathcal{S} & b\mathcal{P} & 0 \\ 0 & 0 & 0 \\ 0 & 0 & 0 \end{bmatrix}, \mathbb{J}[v] \\ &= \begin{bmatrix} 0 & (q_1 + q_2 + r_2) & 0 \\ (s + q_1 + r)\mathcal{P} + b\mathcal{S} & b\mathcal{P} & 0 \\ 0 & -r_2 + r_1\mathcal{Q} & r_1\mathcal{S} + (q_3 + q_1 + \gamma) \end{bmatrix}. \end{aligned} \quad (92)$$

Therefore, the Jacobian matrices of both matrices f and v at disease-free equilibrium point E^0 obtained as (89) are given by

$$\begin{aligned} \mathbb{J}[f] \Big|_{E^0} &= \begin{bmatrix} 0 & \frac{b\theta}{s + q_1 + r} & 0 \\ 0 & 0 & 0 \\ 0 & 0 & 0 \end{bmatrix}, \mathbb{J}[v] \Big|_{E^0} \\ &= \begin{bmatrix} 0 & (q_1 + q_2 + r_2) & 0 \\ \theta & \frac{b\theta}{s + q_1 + r} & 0 \\ 0 & -r_2 & (q_3 + q_1 + \gamma) \end{bmatrix}. \end{aligned} \quad (93)$$

On the other side,

$$\mathbb{J}^{-1}[v] \Big|_{E^0} = \begin{bmatrix} -\frac{b}{(s + q_1 + r)(q_1 + q_2 + r_2)} & \frac{1}{\theta} & 0 \\ \frac{1}{q_1 + q_2 + r_2} & 0 & 0 \\ \frac{r_2}{(q_1 + q_2 + r_2)(q_3 + q_1 + \gamma)} & 0 & \frac{-1}{q_3 + q_1 + \gamma} \end{bmatrix}. \quad (94)$$

By some simple calculations, we get

$$\mathbb{J}[f] \Big|_{E^0} \cdot \mathbb{J}^{-1}[v] \Big|_{E^0} = \begin{bmatrix} \frac{b\theta}{(s + q_1 + r)(q_1 + q_2 + r_2)} & 0 & 0 \\ 0 & 0 & 0 \\ 0 & 0 & 0 \end{bmatrix}. \quad (95)$$

In the final step, the spectral radius of the next generation matrix $(\mathbb{J}[f] \Big|_{E^0} \cdot \mathbb{J}^{-1}[v] \Big|_{E^0})$ is the basic reproduction number R_0 which is given by

$$R_0 = \rho \left(\mathbb{J}[f] \Big|_{E^0} \cdot \mathbb{J}^{-1}[v] \Big|_{E^0} \right) = \frac{b\theta}{(s + q_1 + r)(q_1 + q_2 + r_2)}. \quad (96)$$

In Figures 1–4, we plot the dynamics of R_0 by 3D plots and the contours of the basic production number versus different parameters.

7.3. Endemic Equilibrium Point. As we know, the quantity R_0 is a criterion to measure the transmission potential of a infectious disease during a specific time. Whenever $R_0 > 1$, then the fractal-fractional second-hand smoker model (7) involves an endemic equilibrium point $E^* = (\mathcal{P}^*, \mathcal{S}^*, \mathcal{Q}^*)$. To find this point, we must solve the homogeneous system of equation (88) by considering this claim that all state

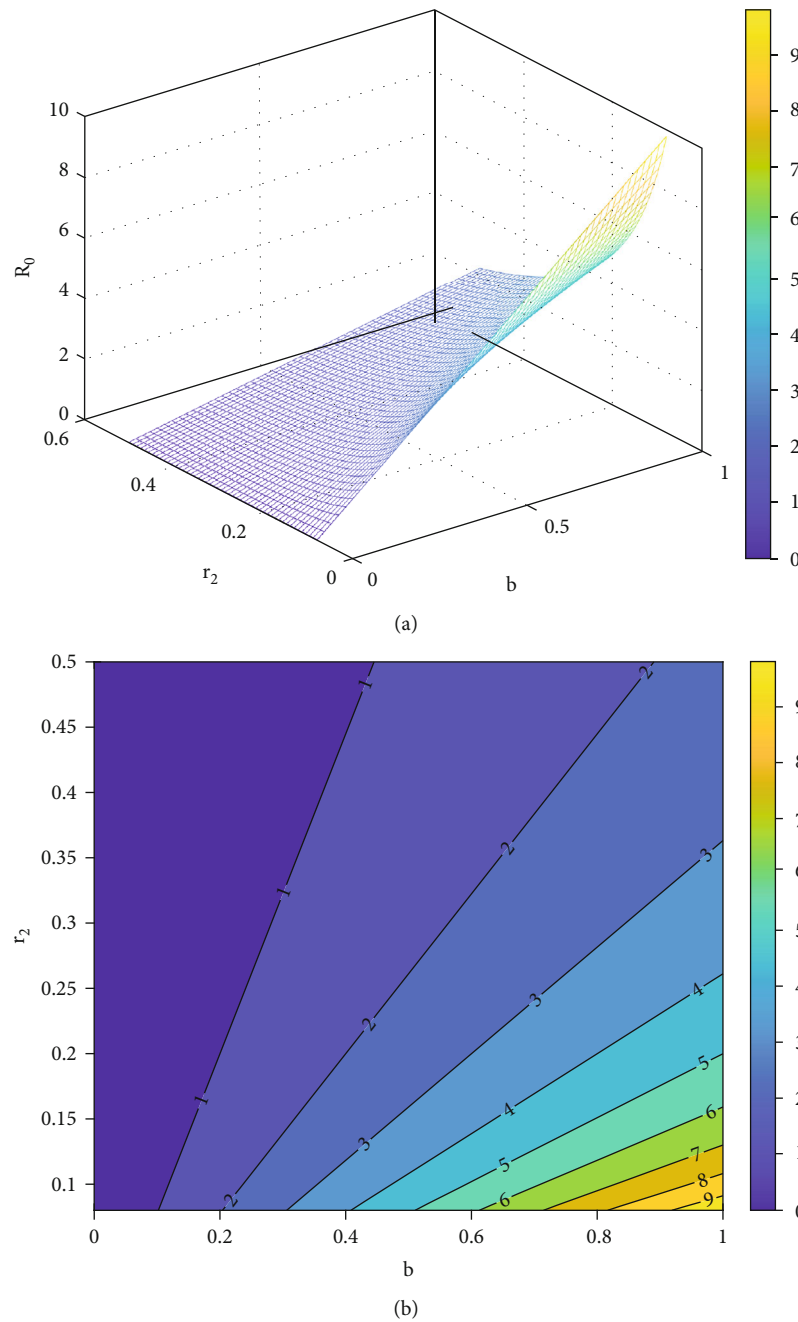


FIGURE 1: The dynamics of R_0 by 3D plot and the contour of R_0 vs. b and r_2 , respectively.

functions $\mathcal{P}(t)$, $\mathcal{S}(t)$, $\mathcal{Q}(t)$ are nonzero. Therefore, from the second equation of (88) and by assuming $\mathcal{S}(t) \neq 0$, we get

$$b\mathcal{P} + r_1\mathcal{Q} = q_1 + q_2 + r_2. \quad (97)$$

Now, we rewrite the first and third equations of (88) as

$$\begin{cases} \theta - [(s + q_1 + r) + b\mathcal{S}]\mathcal{P} = 0, \\ r_2\mathcal{S} - [r_1\mathcal{S} + (q_3 + q_1 + \gamma)]\mathcal{Q} = 0, \end{cases} \quad (98)$$

and we derive the following relations

$$\mathcal{P} = \frac{\theta}{(s + q_1 + r) + b\mathcal{S}}, \quad \mathcal{Q} = \frac{r_2\mathcal{S}}{r_1\mathcal{S} + (q_3 + q_1 + \gamma)}. \quad (99)$$

We substitute above relations into (97) and by assuming the constants $K_1 = s + q_1 + r > 0$, $K_2 = q_1 + q_2 + r_2 > 0$ and $K_3 = q_3 + q_1 + \gamma > 0$, we obtain

$$\frac{b\theta}{K_1 + b\mathcal{S}} + \frac{r_1 r_2 \mathcal{S}}{r_1 \mathcal{S} + K_3} - K_2 = 0. \quad (100)$$

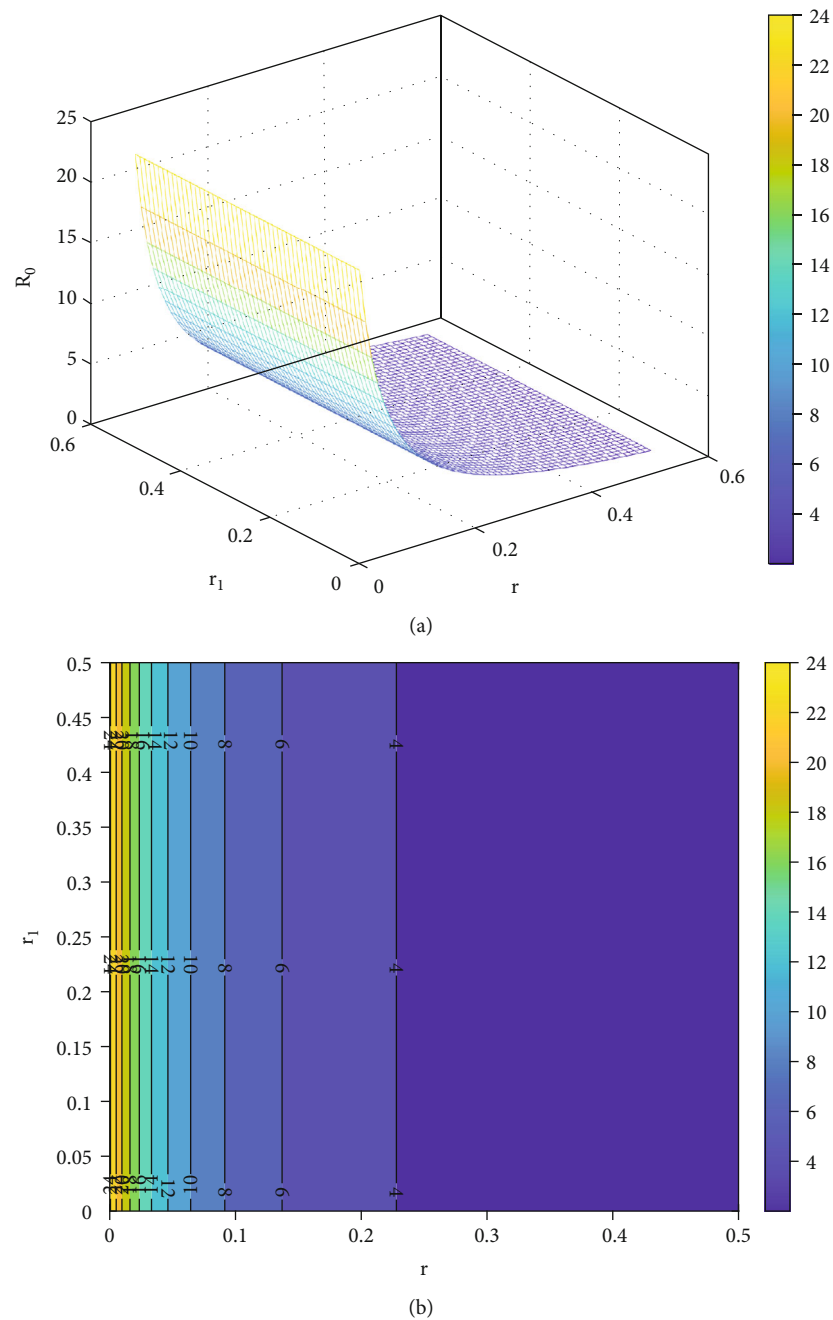


FIGURE 2: The dynamics of R_0 by 3D plot and the contour of R_0 vs. r and r_1 , respectively.

We have

$$\frac{b\theta(r_1\mathcal{S} + K_3) + r_1r_2\mathcal{S}(K_1 + b\mathcal{S}) - K_2(K_1 + b\mathcal{S})(r_1\mathcal{S} + K_3)}{(K_1 + b\mathcal{S})(r_1\mathcal{S} + K_3)} = 0. \quad (101)$$

Since the denominator of the above equation is nonzero, hence

$$b\theta(r_1\mathcal{S} + K_3) + r_1r_2\mathcal{S}(K_1 + b\mathcal{S}) - K_2(K_1 + b\mathcal{S})(r_1\mathcal{S} + K_3) = 0. \quad (102)$$

On the other hand, by the new notation, we know that $R_0 = b\theta/K_1K_2$ and so $K_1K_2R_0 = b\theta$. Thus, from (102) and by some simple calculations, we derive a quadratic equation with respect to \mathcal{S} as

$$(r_1r_2b - r_1bK_2)\mathcal{S}^2 + (r_1r_2K_1 - bK_2K_3 + r_1K_1K_2(R_0 - 1))\mathcal{S} + K_1K_2K_3(R_0 - 1) = 0. \quad (103)$$

Set $Y_1 = r_1br_2 - r_1bK_2$, and

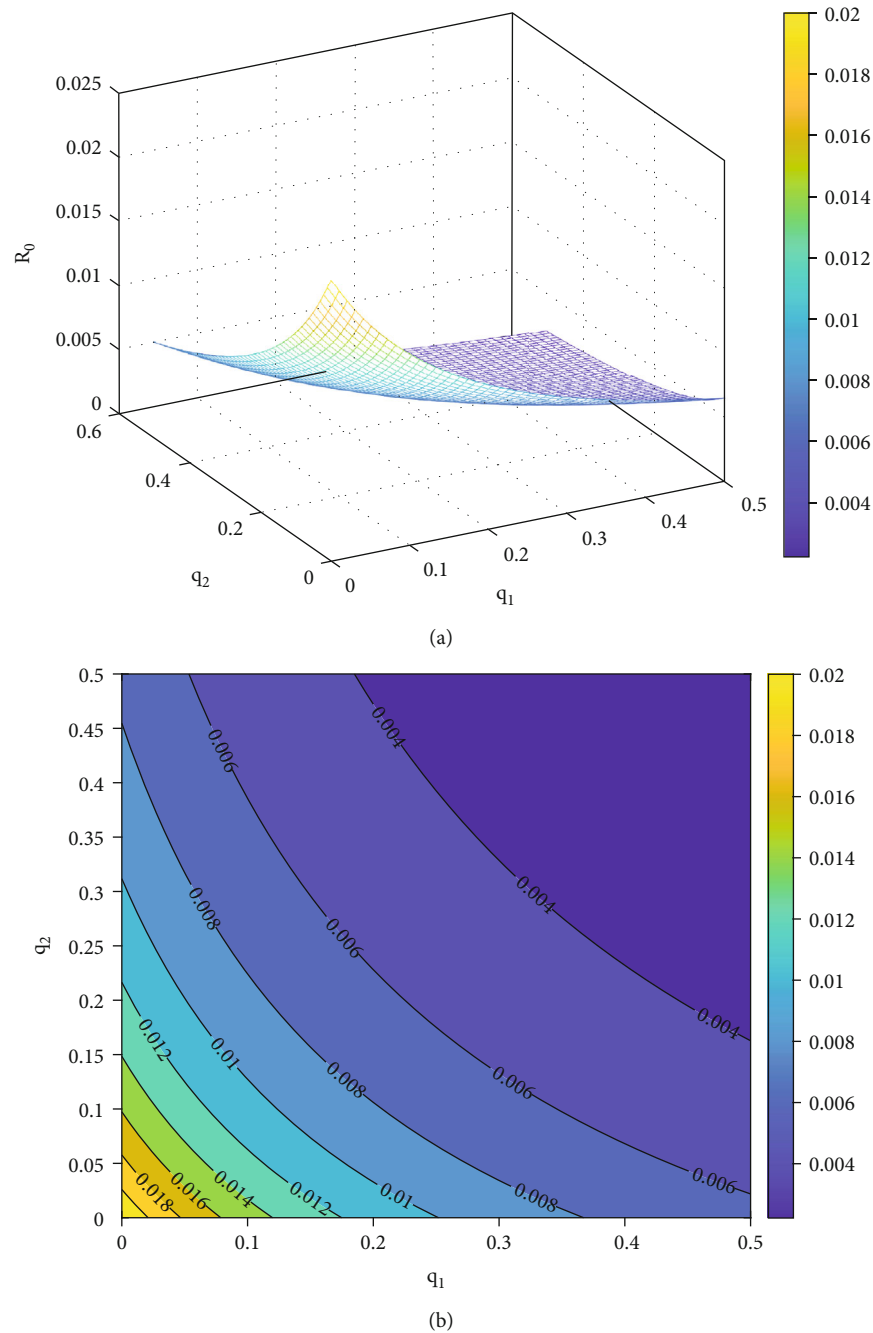


FIGURE 3: The dynamics of R_0 by 3D plot and the contour of R_0 vs. q_1 and q_2 , respectively.

$$Y_2 = r_1 r_2 K_1 - b K_2 K_3 + r_1 K_1 K_2 (R_0 - 1), \quad (104)$$

and $Y_3 = K_1 K_2 K_3 (R_0 - 1)$. Consequently, we get

$$\mathcal{S} = \frac{-Y_2 \pm \sqrt{Y_2^2 - 4Y_1 Y_3}}{2Y_1}. \quad (105)$$

Since $r_1 b r_2 < r_1 b K_2$, thus $Y_1 < 0$ and if $R_0 > 1$, then

$$\mathcal{S}^* = \frac{-Y_2 - \sqrt{Y_2^2 - 4Y_1 Y_3}}{2Y_1}. \quad (106)$$

Simply, \mathcal{P}^* and \mathcal{Q}^* can be obtained by inserting the equation (106) into equation (99), and therefore,

$$\mathcal{P}^* = \frac{\theta}{(s + q_1 + r) + b \left(-Y_2 - \sqrt{Y_2^2 - 4Y_1 Y_3} / 2Y_1 \right)}, \quad (107)$$

$$\mathcal{Q}^* = \frac{r_2 \left(-Y_2 - \sqrt{Y_2^2 - 4Y_1 Y_3} / 2Y_1 \right)}{r_1 \left(-Y_2 - \sqrt{Y_2^2 - 4Y_1 Y_3} / 2Y_1 \right) + (q_3 + q_1 + \gamma)}. \quad (108)$$

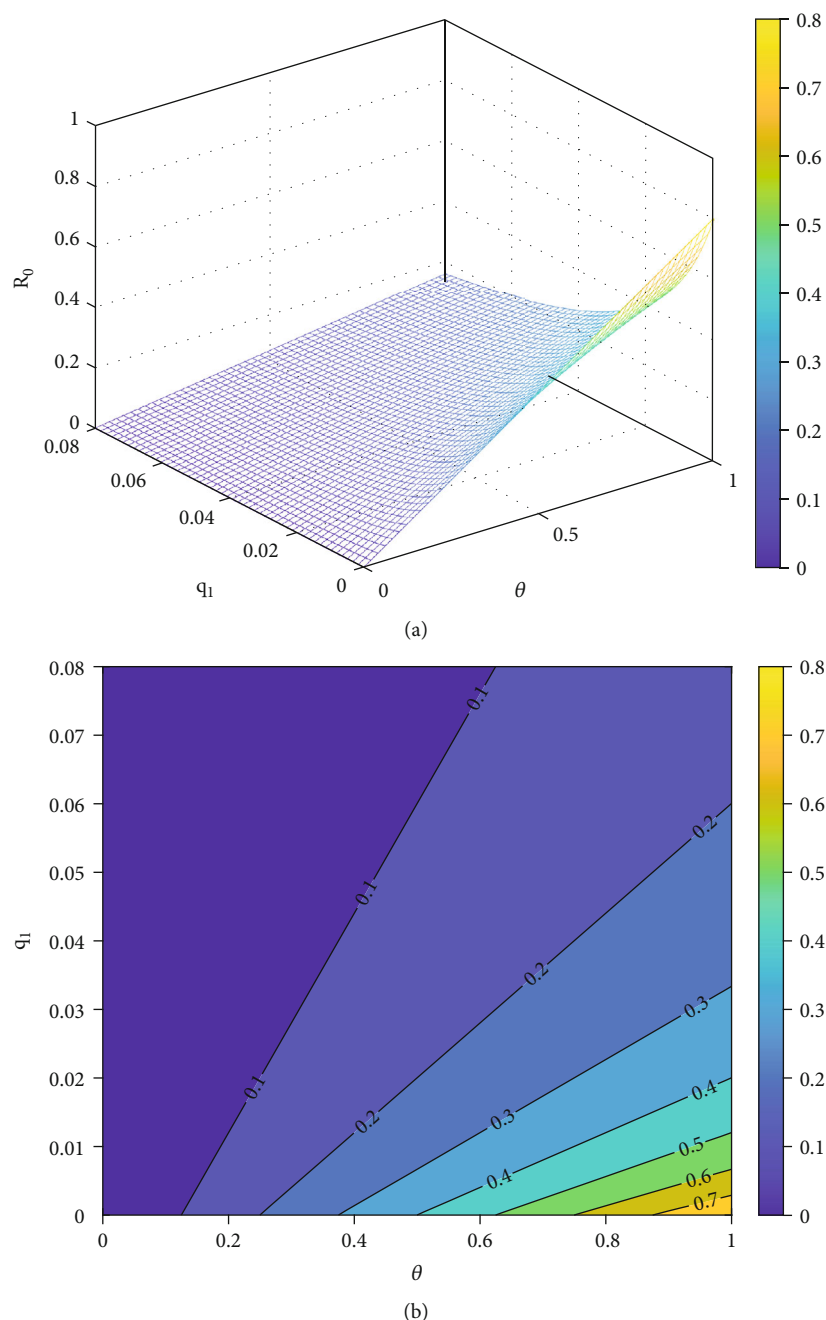


FIGURE 4: The dynamics of R_0 by 3D plot and the contour of R_0 vs. θ and q_1 , respectively.

Theorem 19. If $R_0 > 1$ or $R_0 = 1$ and $r_1 r_2 K_1 > b K_2 K_3$, then there exists $E^* = (\mathcal{P}^*, \mathcal{S}^*, \mathcal{Q}^*)$ as the endemic equilibrium point, where \mathcal{P}^* , \mathcal{S}^* , and \mathcal{Q}^* are as (106)–(108). Also, If $R_0 < 1$, then this point does not exist.

Proof. If $R_0 > 1$, then by the above discussions, $E^* = (\mathcal{P}^*, \mathcal{S}^*, \mathcal{Q}^*)$ exists. If $R_0 = 1$, then $Y_2 = r_1 r_2 K_1 - b K_2 K_3$ and $Y_3 = 0$. In this case, we have

$$\mathcal{S} = \frac{-Y_2 - |Y_2|}{2Y_1}. \quad (109)$$

On the other side, we know that $Y_1 \neq 0$. Hence, if $Y_2 \leq 0$, then $\mathcal{S} = 0$ and if $Y_2 > 0$, then $\mathcal{S} < 0$. These show the existence of the endemic equilibrium point E^* .

On the other side, $R_0 < 1$ gives $-Y_2 > 0$ and $Y_3 < 0$. Thus, either \mathcal{S} is a complex number or a negative real number, and E^* does not exist. \square

In Figures 5 and 6, we show the stability curves of \mathcal{P} , \mathcal{S} , and \mathcal{Q} at endemic equilibrium point E^* for some values of the fractal and fractional orders.

7.4. Local Asymptotic Stability Analysis. In this place, we aim to investigate the local asymptotic stability of the smoke-free

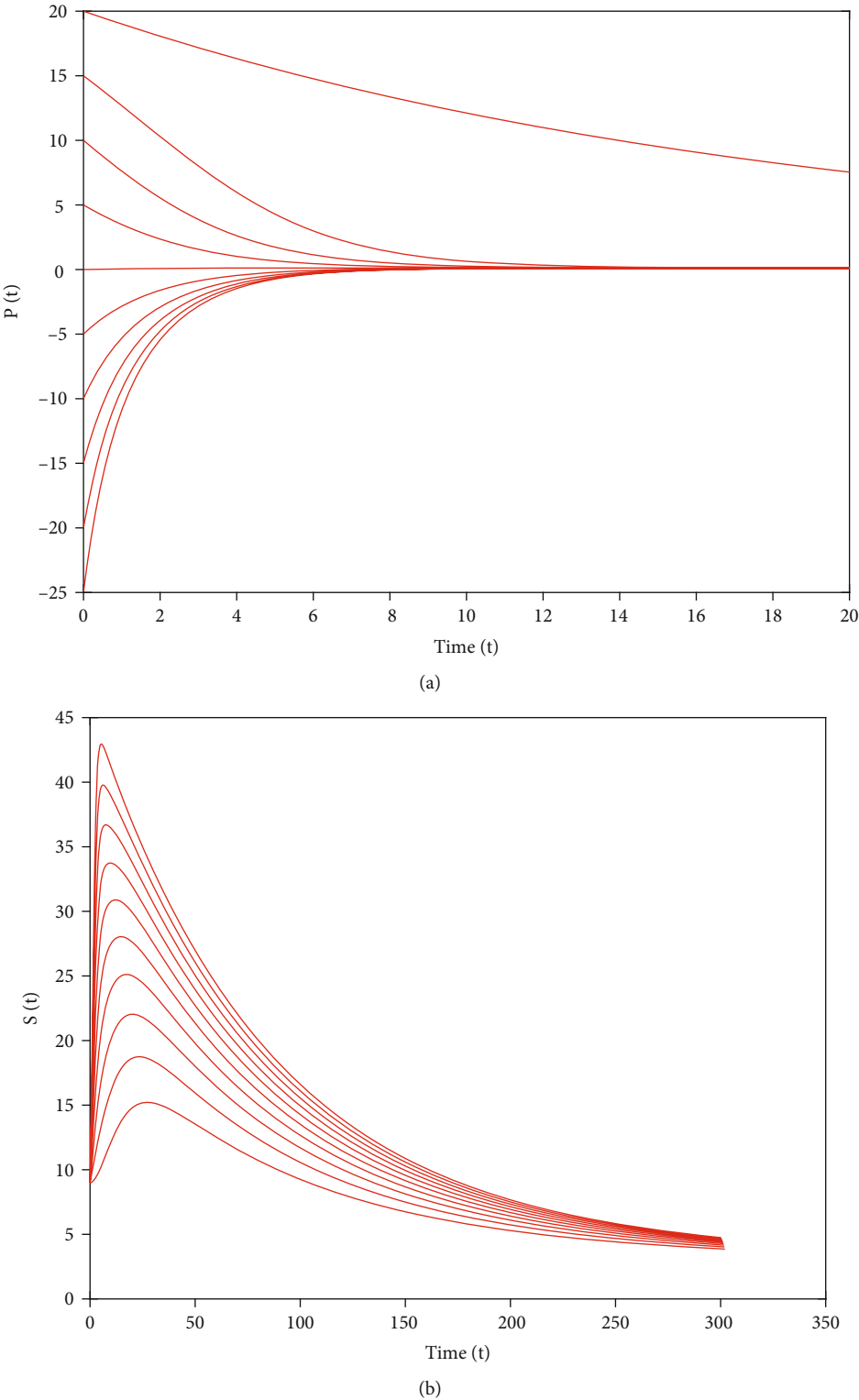
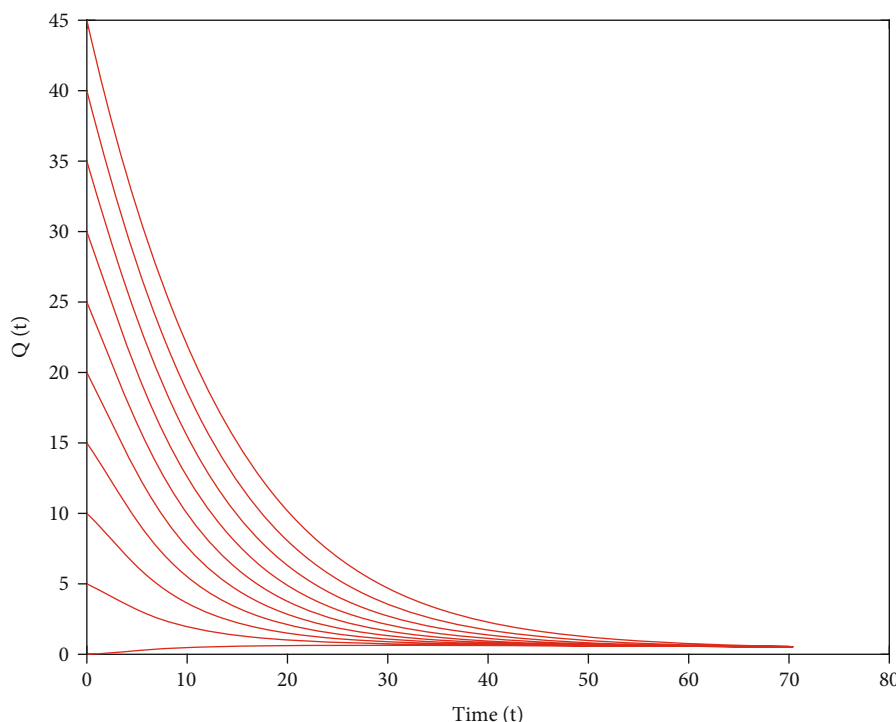


FIGURE 5: The stability curves of $\mathcal{P}(t)$ and $\mathcal{S}(t)$ at E^* for $\omega = 0.97$ and $\nu = 0.5$.

FIGURE 6: The stability curves of $Q(t)$ at E^* for $\omega = 0.97$ and $\nu = 0.5$.

point E^0 found in (89) in relation to the fractal-fractional model (7) of second-hand smokers. First, we obtain the Jacobian matrix of the fractal-fractional system (7) as

$$\mathbb{J} = \begin{bmatrix} -(s+q_1+r) - b\mathcal{S} & -b\mathcal{P} & 0 \\ b\mathcal{S} & b\mathcal{P} + r_1\mathcal{Q} - (q_1+q_2+r_2) & r_1\mathcal{S} \\ 0 & r_2 - r_1\mathcal{Q} & -r_1\mathcal{S} - (q_3+q_1+\gamma) \end{bmatrix}. \quad (110)$$

Theorem 20. *The fractal-fractional model (7) of second-hand smokers is locally asymptotically stable at smoke-free equilibrium point E^0 if all roots of the characteristic polynomial $\det(\mathbb{J}(E^0) - \lambda I) = 0$ are negative or $R_0 < 1$; otherwise, it is unstable.*

Proof. In view of (110), the Jacobian matrix $\mathbb{J}(E^0)$ of the model (7) at smoke-free equilibrium point E^0 is given as

$$\mathbb{J}(E^0) = \begin{bmatrix} -(s+q_1+r) & \frac{-b\theta}{s+q_1+r} & 0 \\ 0 & \frac{b\theta}{s+q_1+r} - (q_1+q_2+r_2) & 0 \\ 0 & r_2 & -(q_3+q_1+\gamma) \end{bmatrix}. \quad (111)$$

By considering the Jacobian matrix (111) and by $\det(\mathbb{J}(E^0) - \lambda I) = 0$, the characteristic polynomial becomes

$$(\lambda + s + q_1 + r)(\lambda + q_3 + q_1 + \gamma) \left(\lambda - \left(\frac{b\theta}{s + q_1 + r} - (q_1 + q_2 + r_2) \right) \right) = 0. \quad (112)$$

The roots of the above polynomial are

$$\lambda_1 = -(s + q_1 + r), \lambda_2 = -(q_3 + q_1 + \gamma), \lambda_3 = \frac{b\theta}{s + q_1 + r} - (q_1 + q_2 + r_2). \quad (113)$$

Since all parameters are assumed to be positive, we clearly have $\lambda_1 < 0$ and $\lambda_2 < 0$. On the other hand, if $R_0 < 1$, then $R_0 - 1 < 0$. So, we can write

$$\frac{b\theta}{(s + q_1 + r)(q_1 + q_2 + r_2)} < 1. \quad (114)$$

Hence,

$$\frac{b\theta}{(s + q_1 + r)} < (q_1 + q_2 + r_2). \quad (115)$$

Consequently, $\lambda_3 = b\theta/(s + q_1 + r) - (q_1 + q_2 + r_2) < 0$. Thus, all of roots are negative, and so the fractal-fractional second-hand smoker model (7) is locally asymptotically stable around the smoke-free equilibrium point E^0 . This completes the proof. \square

7.5. Sensitivity Analysis. To find out how sensitive the parameters in each model are to the transmission of infections or diseases, the authors use a criterion introduced by Chitnis et al. [49]. Here, to obtain the sensitivity of R_0 in terms of each of its parameters, we compute the partial derivative with respect to every parameter in the reproduction number. In other words, if p is an arbitrary parameter, then the sensitivity index of R_0 versus p is calculated by

$$\mathbb{S}_p^{\mathcal{R}_0} = \frac{p}{\mathcal{R}_0} \left[\frac{\partial \mathcal{R}_0}{\partial p} \right]. \quad (116)$$

Now, according to the above relation, we have

$$\mathbb{S}_b^{\mathcal{R}_0} = \frac{b}{\mathcal{R}_0} \left[\frac{\theta}{(q_1 + r_2 + q_2)(q_1 + r + s)} \right] > 0, \quad (117)$$

$$\mathbb{S}_\theta^{\mathcal{R}_0} = \frac{\theta}{\mathcal{R}_0} \left[\frac{b}{(q_1 + r_2 + q_2)(q_1 + r + s)} \right] > 0, \quad (118)$$

$$\mathbb{S}_s^{\mathcal{R}_0} = \frac{s}{\mathcal{R}_0} \left[-\frac{b\theta}{(q_1 + r_2 + q_2)(q_1 + r + s)^2} \right] < 0, \quad (119)$$

$$\mathbb{S}_{q_1}^{\mathcal{R}_0} = \frac{q_1}{\mathcal{R}_0} \left[-\frac{b\theta}{(q_1 + q_2 + r_2)(q_1 + r + s)^2} - \frac{b\theta}{(q_1 + r_2 + q_2)^2 (q_1 + r + s)} \right] < 0, \quad (120)$$

$$\mathbb{S}_r^{\mathcal{R}_0} = \frac{r}{\mathcal{R}_0} \left[-\frac{b\theta}{(q_1 + r_2 + q_2)(q_1 + r + s)^2} \right] < 0, \quad (121)$$

$$\mathbb{S}_{q_2}^{\mathcal{R}_0} = \frac{q_2}{\mathcal{R}_0} \left[-\frac{b\theta}{(q_1 + r_2 + q_2)^2 (q_1 + r + s)} \right] < 0, \quad (122)$$

$$\mathbb{S}_{r_2}^{\mathcal{R}_0} = \frac{r_2}{\mathcal{R}_0} \left[-\frac{b\theta}{(q_1 + r_2 + q_2)^2 (q_1 + r + s)} \right] < 0. \quad (123)$$

The numeric values for sensitivity indices (120) are given in Table 1.

In Figure 7, when the sign of sensitivity index is positive, then each increase (decrease) in the value of parameters (assuming the remaining parameters to be constant) increases (decreases) the value of R_0 . The negative sign in this index gives the inverse result for R_0 . In the sensitivity analysis of our second-hand smoker model (7), it is observed that R_0 increases by increasing the values of b, θ and decreases by increasing the values of s, q_1, r, q_2, r_2 . For example, $\mathbb{S}_{q_1}^{\mathcal{R}_0} = -0.0061$ means that an increase in q_1 by 10% decreases R_0 by 0.061%. Therefore, to reduce the spread of infections, those parameters having negative sensitivity indices must be minimized in the environment.

8. Numerical scheme

In this section, we describe the numerical scheme in relation to the fractal-fractional model of second-hand smoker (7).

TABLE 1: Sensitivity of the R_0 versus proposed parameters.

Parameter	\mathbb{S}	Value	Parameter	\mathbb{S}	Value
b	$\mathbb{S}_b^{\mathcal{R}_0}$	+1.0000	θ	$\mathbb{S}_\theta^{\mathcal{R}_0}$	+1.0000
s	$\mathbb{S}_s^{\mathcal{R}_0}$	-9.1621e-05	q_1	$\mathbb{S}_{q_1}^{\mathcal{R}_0}$	-0.0061
r	$\mathbb{S}_r^{\mathcal{R}_0}$	-0.0366	q_2	$\mathbb{S}_{q_2}^{\mathcal{R}_0}$	-0.0018
r_2	$\mathbb{S}_{r_2}^{\mathcal{R}_0}$	-4.0813e-04			

For this, we have taken help from the technique regarding two-step Lagrange polynomials known as the fractional Adams-Bashforth (AB) method [50]. To begin this process, we present the numerical method of fractal-fractional integral equation (16) using a new approach at t_{n+1} . In other words, we discretize the mentioned equation (16) for $t = t_{n+1}$, and we have

$$\begin{cases} \mathcal{P}(t_{n+1}) = \mathcal{P}_0 + \frac{\nu}{\Gamma(\omega)} \int_0^{t_{n+1}} (t_{n+1} - \mathfrak{w})^{\omega-1} \mathcal{H}_1(\mathfrak{w}) d\mathfrak{w}, \\ \mathcal{S}(t_{n+1}) = \mathcal{S}_0 + \frac{\nu}{\Gamma(\omega)} \int_0^{t_{n+1}} (t_{n+1} - \mathfrak{w})^{\omega-1} \mathcal{H}_2(\mathfrak{w}) d\mathfrak{w}, \\ \mathcal{Q}(t_{n+1}) = \mathcal{Q}_0 + \frac{\nu}{\Gamma(\omega)} \int_0^{t_{n+1}} (t_{n+1} - \mathfrak{w})^{\omega-1} \mathcal{H}_3(\mathfrak{w}) d\mathfrak{w}, \end{cases} \quad (124)$$

where

$$\begin{cases} \mathcal{H}_1(\mathfrak{w}) = \mathfrak{w}^{\nu-1} \mathbb{W}_1(\mathfrak{w}, \mathcal{P}(\mathfrak{w}), \mathcal{S}(\mathfrak{w}), \mathcal{Q}(\mathfrak{w})), \\ \mathcal{H}_2(\mathfrak{w}) = \mathfrak{w}^{\nu-1} \mathbb{W}_2(\mathfrak{w}, \mathcal{P}(\mathfrak{w}), \mathcal{S}(\mathfrak{w}), \mathcal{Q}(\mathfrak{w})), \\ \mathcal{H}_3(\mathfrak{w}) = \mathfrak{w}^{\nu-1} \mathbb{W}_3(\mathfrak{w}, \mathcal{P}(\mathfrak{w}), \mathcal{S}(\mathfrak{w}), \mathcal{Q}(\mathfrak{w})). \end{cases} \quad (125)$$

By approximating above integrals, we get

$$\begin{cases} \mathcal{P}(t_{n+1}) = \mathcal{P}_0 + \frac{\nu}{\Gamma(\omega)} \sum_{l=0}^n \int_{t_l}^{t_{l+1}} (t_{n+1} - \mathfrak{w})^{\omega-1} \mathcal{H}_1(\mathfrak{w}) d\mathfrak{w}, \\ \mathcal{S}(t_{n+1}) = \mathcal{S}_0 + \frac{\nu}{\Gamma(\omega)} \sum_{l=0}^n \int_{t_l}^{t_{l+1}} (t_{n+1} - \mathfrak{w})^{\omega-1} \mathcal{H}_2(\mathfrak{w}) d\mathfrak{w}, \\ \mathcal{Q}(t_{n+1}) = \mathcal{Q}_0 + \frac{\nu}{\Gamma(\omega)} \sum_{l=0}^n \int_{t_l}^{t_{l+1}} (t_{n+1} - \mathfrak{w})^{\omega-1} \mathcal{H}_3(\mathfrak{w}) d\mathfrak{w}. \end{cases} \quad (126)$$

In the sequel, we approximate the functions $\mathcal{H}_1(\mathfrak{w}), \mathcal{H}_2(\mathfrak{w}), \mathcal{H}_3(\mathfrak{w})$ introduced by (125), on the interval $[t_l, t_{l+1}]$ via

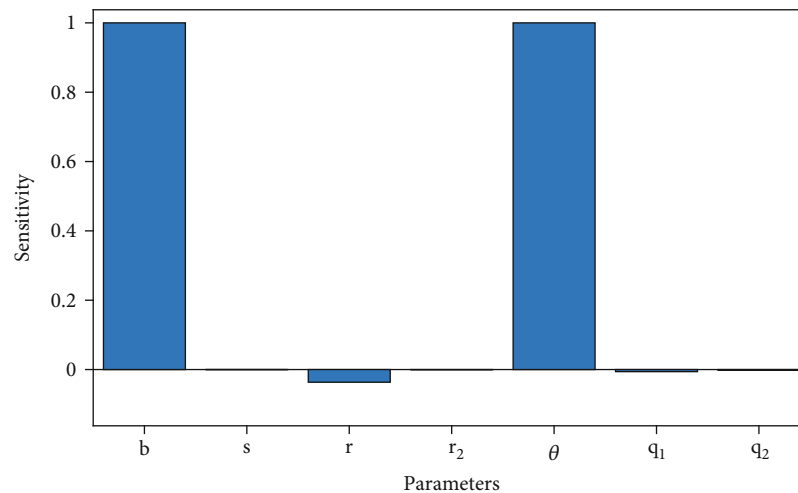


FIGURE 7: Global sensitivity analysis of model (7) based on R_0 (96) and sensitivity analysis (120).

two-step Lagrange interpolation polynomials with the step size $h = t_l - t_{l-1}$ as

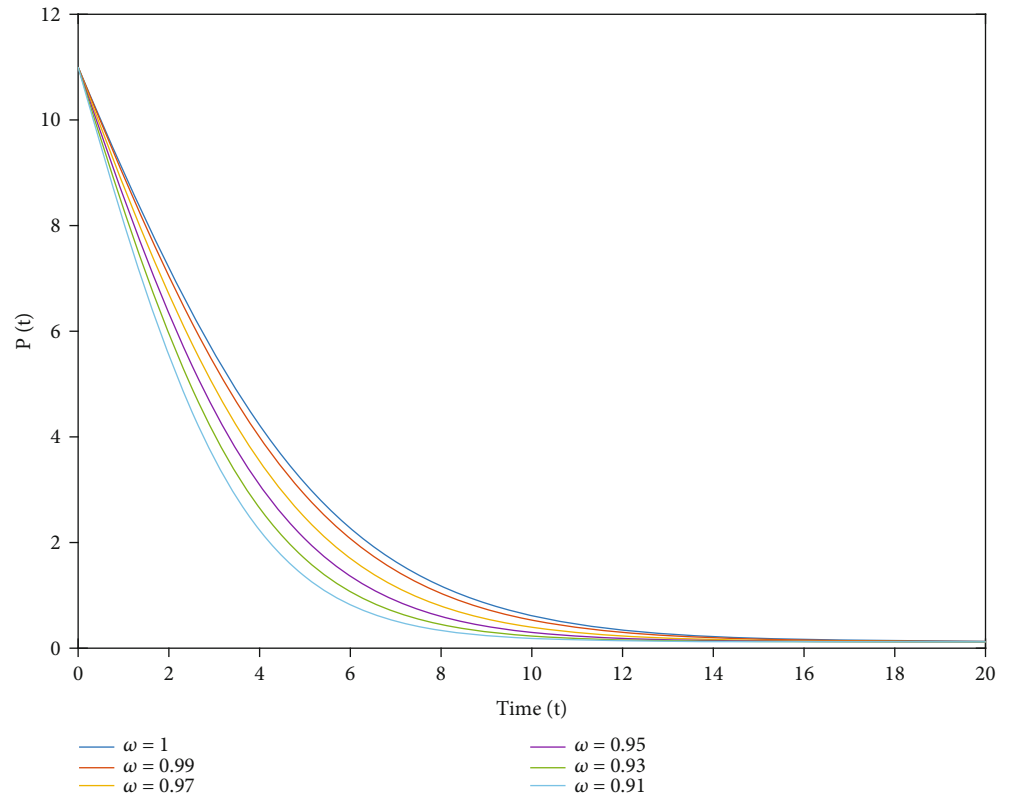
$$\begin{aligned}\mathcal{H}_{1,l}^*(w) &\approx \frac{w - t_{l-1}}{h} t_l^{v-1} \mathbb{W}_1(w, \mathcal{P}_l, \mathcal{S}_l, \mathcal{Q}_l) - \frac{w - t_l}{h} t_{l-1}^{v-1} \mathbb{W}_1(w_{l-1}, \mathcal{P}_{l-1}, \mathcal{S}_{l-1}, \mathcal{Q}_{l-1}), \\ \mathcal{H}_{2,l}^*(w) &\approx \frac{w - t_{l-1}}{h} t_l^{v-1} \mathbb{W}_2(w, \mathcal{P}_l, \mathcal{S}_l, \mathcal{Q}_l) - \frac{w - t_l}{h} t_{l-1}^{v-1} \mathbb{W}_2(w_{l-1}, \mathcal{P}_{l-1}, \mathcal{S}_{l-1}, \mathcal{Q}_{l-1}), \\ \mathcal{H}_{3,l}^*(w) &\approx \frac{w - t_{l-1}}{h} t_l^{v-1} \mathbb{W}_3(w, \mathcal{P}_l, \mathcal{S}_l, \mathcal{Q}_l) - \frac{w - t_l}{h} t_{l-1}^{v-1} \mathbb{W}_3(w_{l-1}, \mathcal{P}_{l-1}, \mathcal{S}_{l-1}, \mathcal{Q}_{l-1}).\end{aligned}\quad (127)$$

Then, we have

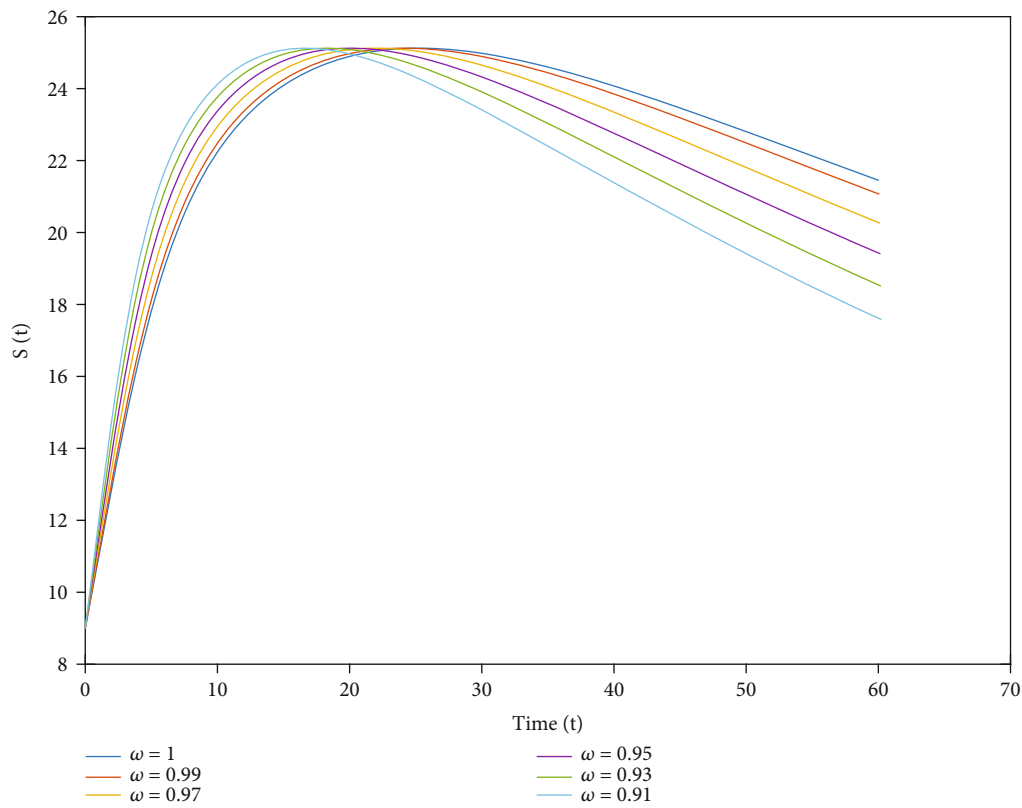
$$\begin{cases} \mathcal{P}(t_{n+1}) = \mathcal{P}_0 + \frac{v}{\Gamma(\omega)} \sum_{l=0}^n \int_{t_l}^{t_{l+1}} (t_{n+1} - w)^{\omega-1} \mathcal{H}_{1,l}^*(w) dw, \\ \mathcal{S}(t_{n+1}) = \mathcal{S}_0 + \frac{v}{\Gamma(\omega)} \sum_{l=0}^n \int_{t_l}^{t_{l+1}} (t_{n+1} - w)^{\omega-1} \mathcal{H}_{2,l}^*(w) dw, \\ \mathcal{Q}(t_{n+1}) = \mathcal{Q}_0 + \frac{v}{\Gamma(\omega)} \sum_{l=0}^n \int_{t_l}^{t_{l+1}} (t_{n+1} - w)^{\omega-1} \mathcal{H}_{3,l}^*(w) dw. \end{cases}\quad (128)$$

By evaluating above integrals directly, the numerical solutions of the given fractal-fractional model of second-hand smoker (7) are given by

$$\begin{aligned}\mathcal{P}_{n+1} &= \mathcal{P}_0 + \frac{vh^\omega}{\Gamma(\omega+2)} \sum_{l=0}^n \left[t_l^{v-1} \mathbb{W}_1(t_l, \mathcal{P}_l, \mathcal{S}_l, \mathcal{Q}_l) Y_{(n,l)} - t_{l-1}^{v-1} \mathbb{W}_1(t_{l-1}, \mathcal{P}_{l-1}, \mathcal{S}_{l-1}, \mathcal{Q}_{l-1}) \hat{Y}_{(n,l)} \right], \\ \mathcal{S}_{n+1} &= \mathcal{S}_0 + \frac{vh^\omega}{\Gamma(\omega+2)} \sum_{l=0}^n \left[t_l^{v-1} \mathbb{W}_2(t_l, \mathcal{P}_l, \mathcal{S}_l, \mathcal{Q}_l) Y_{(n,l)} - t_{l-1}^{v-1} \mathbb{W}_2(t_{l-1}, \mathcal{P}_{l-1}, \mathcal{S}_{l-1}, \mathcal{Q}_{l-1}) \hat{Y}_{(n,l)} \right], \\ \mathcal{Q}_{n+1} &= \mathcal{Q}_0 + \frac{vh^\omega}{\Gamma(\omega+2)} \sum_{l=0}^n \left[t_l^{v-1} \mathbb{W}_3(t_l, \mathcal{P}_l, \mathcal{S}_l, \mathcal{Q}_l) Y_{(n,l)} - t_{l-1}^{v-1} \mathbb{W}_3(t_{l-1}, \mathcal{P}_{l-1}, \mathcal{S}_{l-1}, \mathcal{Q}_{l-1}) \hat{Y}_{(n,l)} \right],\end{aligned}\quad (129)$$



(a)



(b)

FIGURE 8: The simulation of the functions $\mathcal{P}(t)$ and $\mathcal{S}(t)$ during the time t for different fractional orders $\omega = 1, 0.99, 0.97, 0.95, 0.93, 0.91$ and fractal dimension $\nu = 0.99$.

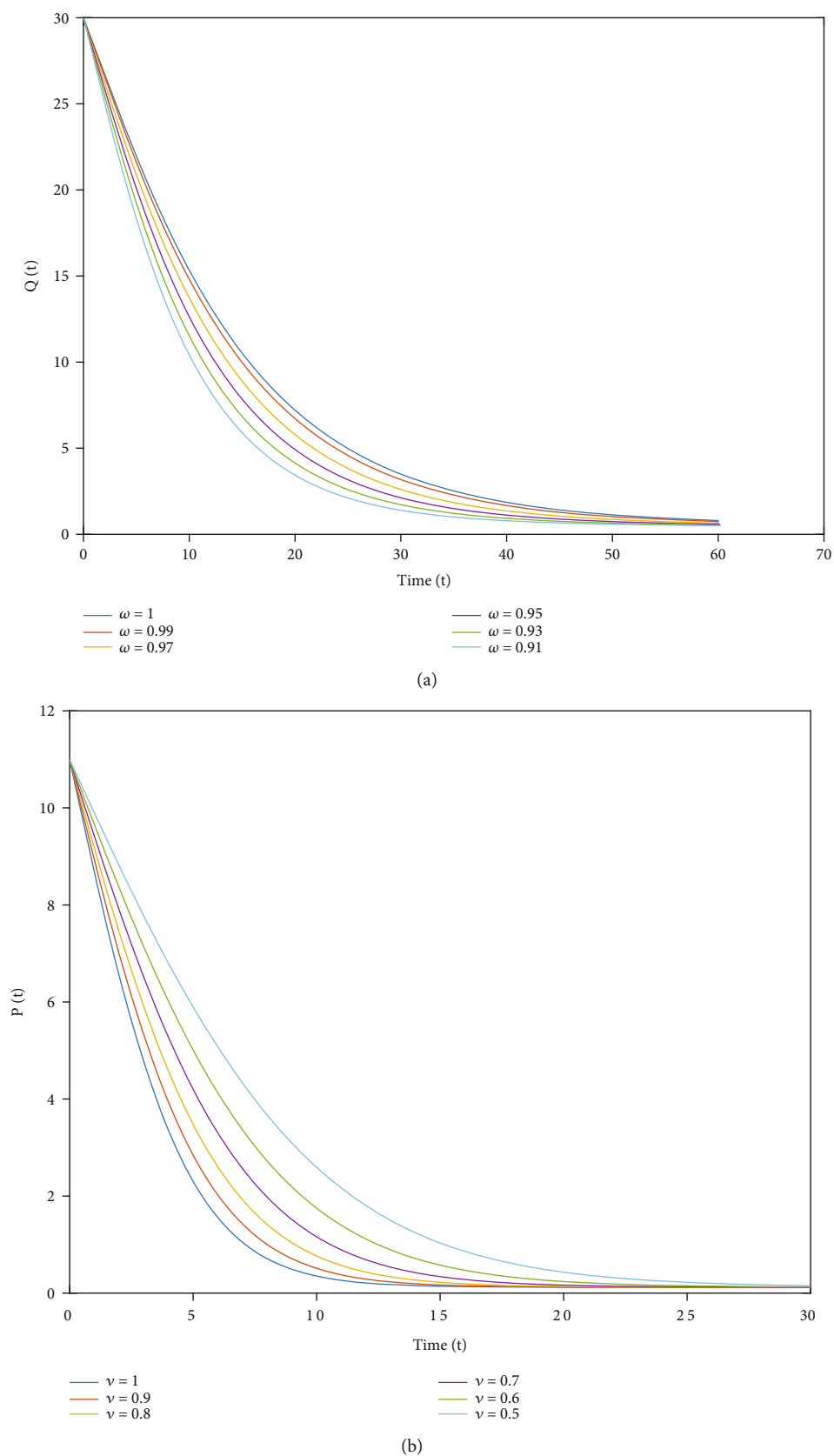


FIGURE 9: (a) The simulation of the function $Q(t)$ during the time t for different fractional orders $\omega = 1, 0.99, 0.97, 0.95, 0.93, 0.91$ and fractal dimension $\nu = 0.99$. (b) The simulation of the function $P(t)$ during the time t for different fractal dimensions $\nu = 1, 0.9, 0.8, 0.7, 0.6, 0.5$ and fractional order $\omega = 0.97$.

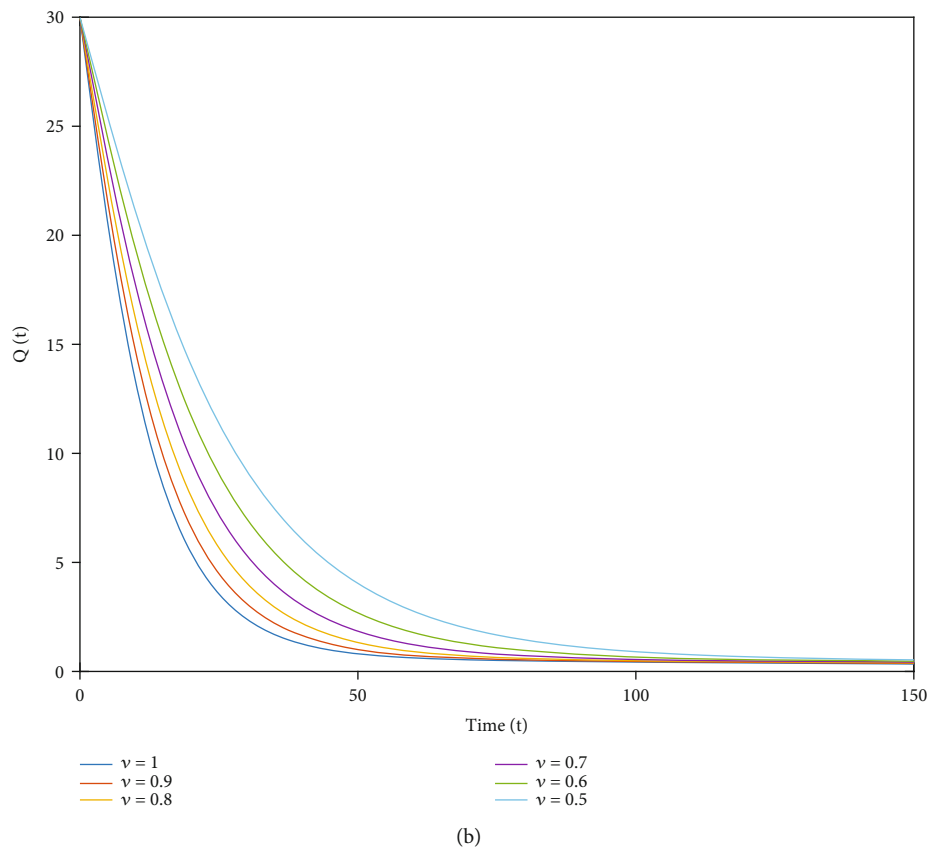
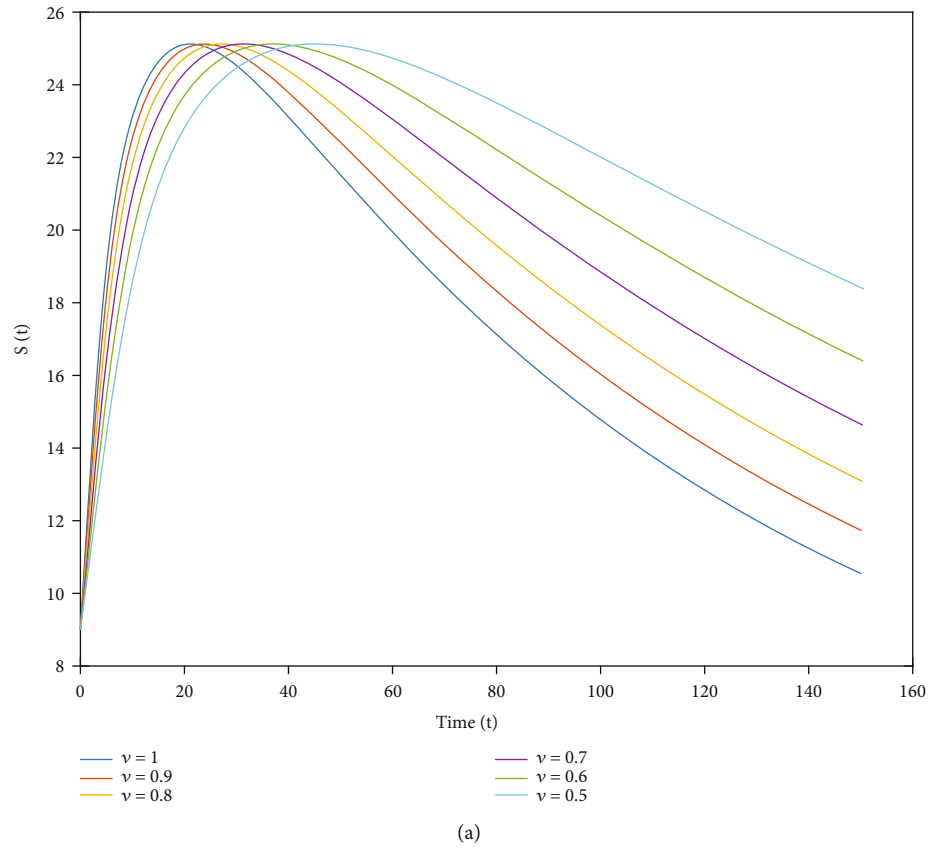


FIGURE 10: The simulation of the functions $\mathcal{S}(t)$ and $\mathcal{Q}(t)$ during the time t for different fractal dimensions $\nu = 1, 0.9, 0.8, 0.7, 0.6, 0.5$ and fractional order $\omega = 0.97$.

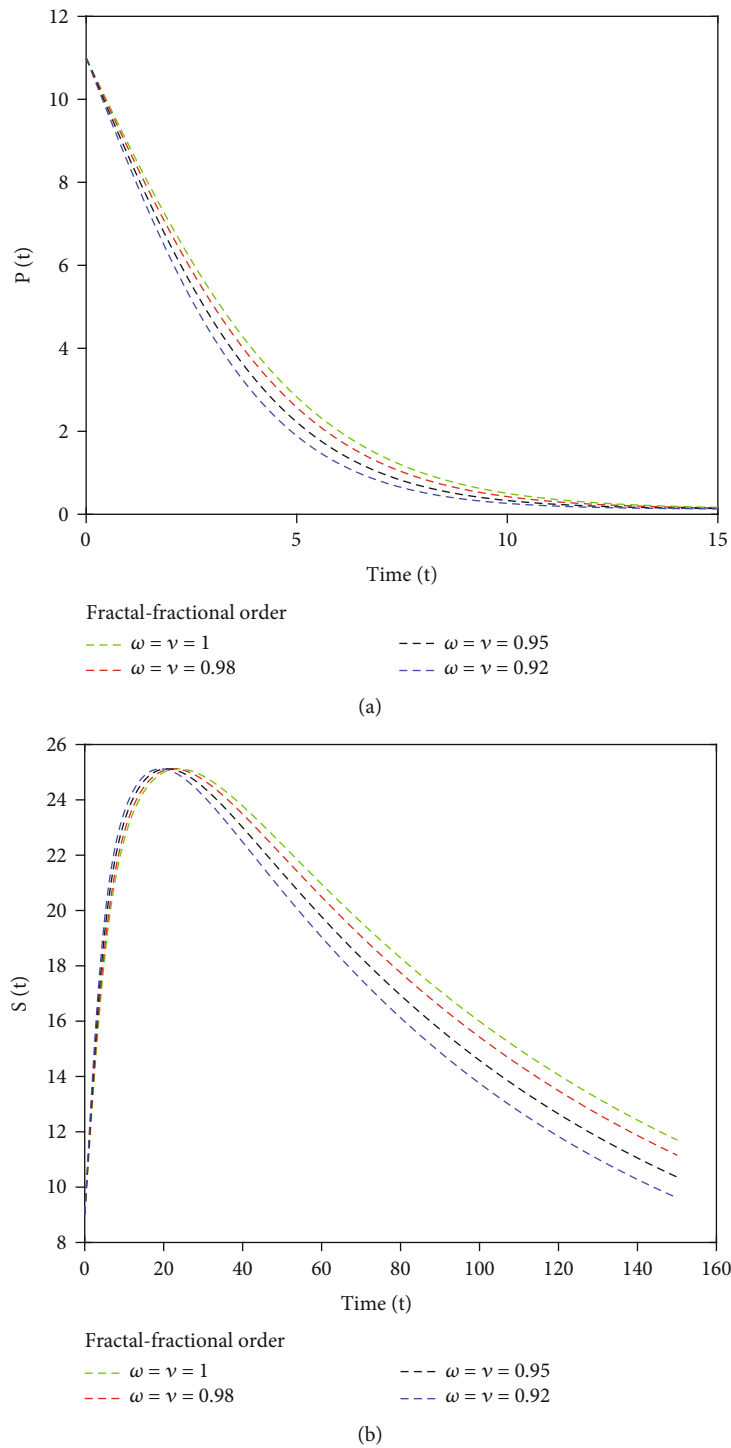


FIGURE 11: The simulation of the functions $\mathcal{P}(t)$ and $\mathcal{S}(t)$ during the time t for fractal dimensions and fractional orders $\omega = \nu = 1, 0.98, 0.95, 0.92$.

where

$$\begin{aligned}
 Y_{(n,l)} &= (n+1-l)^\omega (n-l+2+\omega) - (n-l)^\omega (n-l+2+2\omega), \\
 \hat{Y}_{(n,l)} &= (n+1-l)^{\omega+1} - (n-l)^\omega (n-l+1+\omega),
 \end{aligned}
 \tag{130}$$

where ω is the fractional order of the given fractal-fractional system (7).

9. Simulations

In this section, we simulate and discuss the behavior of the model based on some parameters provided by [45].

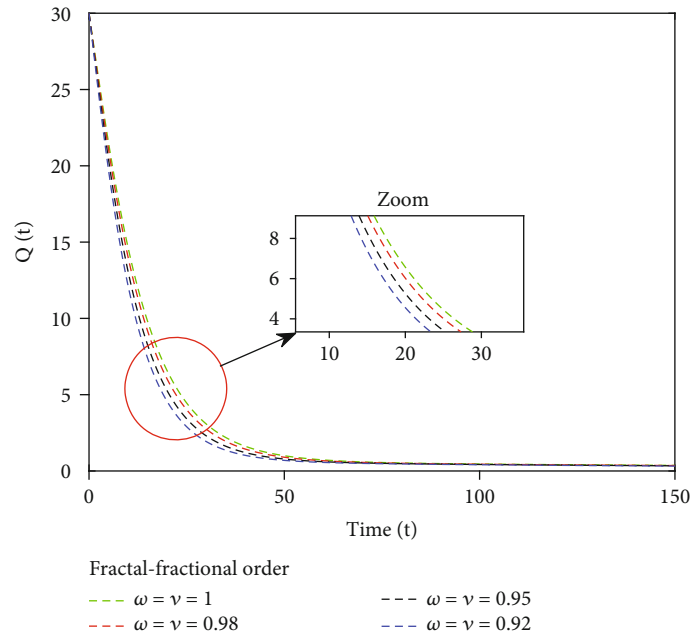


FIGURE 12: The simulation of the function $Q(t)$ during the time t for fractal dimensions and fractional orders $\omega = \nu = 1, 0.98, 0.95, 0.92$.

According to this source, we take $\theta = 0.3$, $s = 0.01$, $q_1 = 0.035$, $r = 0.2$, $b = 0.9001$, $r_1 = 0.009$, $q_2 = 0.01$, $r_2 = 0.01$, $q_3 = 0.1$, and $\gamma = 0.1$. Finally, the initial values for state functions are assumed as $\mathcal{P}(0) = 11$, $\mathcal{S}(0) = 9$, $\mathcal{Q}(0) = 30$. In different figures, we will show the behaviors of three state functions $\mathcal{P}, \mathcal{S}, \mathcal{Q}$ by assuming different values for the fractal order $\nu = 1, 0.9, 0.8, 0.7, 0.6, 0.5$ and fractional orders $\omega = 1.00, 0.99, 0.97, 0.95, 0.93, 0.91$.

More precisely, in Figure 8(a), we see the simulation for different fractional orders $\omega = 1.00, 0.99, 0.97, 0.95, 0.93, 0.91$ and fractal order $\nu = 0.99$ of the function $\mathcal{P}(t)$ in which the rate of population who addicts to tobacco increases with time t , while in Figure 8(b), the simulation of the function $\mathcal{S}(t)$ for the same values of fractal dimension $\nu = 0.99$ and fractional orders $\omega = 1.00, 0.99, 0.97, 0.95, 0.93, 0.91$ shows an increase of addiction to tobacco in the population $\mathcal{S}(t)$ by increasing the time t .

In Figure 9(a), we see the simulation for fractional orders $\omega = 1.00, 0.99, 0.97, 0.95, 0.93, 0.91$ and fractal order $\nu = 0.99$ of the function $\mathcal{Q}(t)$ in which the rate of population who quitting tobacco decreases, while in Figure 9(b), the simulation of the function $\mathcal{P}(t)$ for different fractal orders $\nu = 1, 0.9, 0.8, 0.7, 0.6, 0.5$ and fractional order $\omega = 0.97$ shows an increase in addiction to tobacco in the population at risk.

In Figure 10, we see the simulation for different fractal orders $\nu = 1, 0.9, 0.8, 0.7, 0.6, 0.5$ of the functions $\mathcal{S}(t)$ and $\mathcal{Q}(t)$ for fractional order $\omega = 0.97$ in which the addiction to tobacco increases but the population quitting tobacco decreases.

On the other hand, to see the effect of fractional order and fractal dimension simultaneously, we choose different values for these two parameters as $\omega = \nu = 1, 0.98, 0.95, 0.92$. In Figure 11(a), the simulation of the function $\mathcal{P}(t)$ and (Figure 11(b)) the simulation of the function $\mathcal{S}(t)$ during

the time t are plotted. We see that the change in the behavior of curves when the fractal dimension ν and fractional order ω decreases, then the slope of curves increases and finally, the curves reach to a stable status. We see similar behavior for the function $\mathcal{P}(t)$ in Figure 12.

10. Conclusions

Due to the destructive effects of smoking and its resulting smoke on the health of the people in the community, in the present manuscript, we designed a mathematical model of secondhand smokers (SHS) based on three different compartments of the smoker and nonsmoker population and analyzed it numerically and analytically. To model this system, we applied new derivatives entitled the fractal-fractional derivatives with power-law-type kernel. The existence section was proved by ϕ - ψ -contractions and compact operators, and the Banach principle for usual contractions was used for proving the uniqueness result. The stability notion was investigated for solutions of the fractal-fractional SHS-model (7). The steady-state analysis including calculation of equilibrium points and basic reproduction number R_0 was done, and then we compared the sensitivity of the fractal-fractional SHS-system with each parameter. For numerical simulation, the Adams-Bashforth (AB) method was used and simulated the graphs with the help of real data. The effects of each parameter on the overall result of the calculations showed the increase or decrease in the harmful effect of cigarette smoke on people's health. Along with these results, we see accurate and better simulations via the fractal-fractional operators. Our graphs and data showed that our analysis on real data for different fractal dimensions and fractional orders yield similar results in comparison to classical operators. In the next works, we

can conduct comparative research on different fractal-fractional with exponential decay and power-law type kernels.

Data Availability

Data sharing is not applicable to this article as no datasets were generated or analyzed during the current study.

Conflicts of Interest

The authors declare that they have no competing interests.

Authors' Contributions

The authors declare that the study was realized in collaboration with equal responsibility. All authors read and approved the final manuscript.

Acknowledgments

The first and second authors would like to thank Azarbaijan Shahid Madani University. Also, J. Alzabut expresses his sincere thanks to Prince Sultan University and OSTİM Technical University for their endless support.

References

- [1] World Health Organization, *Protection from exposure to secondhand tobacco smoke, policy recommendations*, World Health Organization, Geneva, 2007.
- [2] J. M. B. Myers, G. K. K. Hershey, R. Deka et al., "Asking the right questions to ascertain early childhood secondhand smoke exposures," *The Journal of Pediatrics*, vol. 160, no. 6, pp. 1050–1051, 2012.
- [3] J. Kusel, B. Timm, and I. Lockhart, "The impact of smoking in the home on the health outcomes of non-smoker occupants in the UK," *Tobacco Induced Diseases*, vol. 11, no. 1, pp. 3–10, 2013.
- [4] X. Zhang, S. X. G. Yang et al., "Association of passive smoking by husbands with prevalence of stroke among Chinese women nonsmokers," *American Journal of Epidemiology*, vol. 161, no. 3, pp. 213–218, 2005.
- [5] S. G. Grant, "Qualitatively and quantitatively similar effects of active and passive maternal tobacco smoke exposure on *in utero* mutagenesis at the *HPRT* locus," *BMC Pediatrics*, vol. 5, no. 1, p. 20, 2005.
- [6] R. Otsuka, H. Watanabe, K. Hirata et al., "Acute effects of passive smoking on the coronary circulation in healthy young adults," *The Journal of the American Medical Association*, vol. 286, no. 4, pp. 436–441, 2001.
- [7] N. Lubick, "Smoking and secondhand smoke: global estimate of SHS burden," *Environmental Health Perspectives*, vol. 119, no. 2, pp. A66–A67, 2011.
- [8] A. Burton, "Does the smoke ever really clear? Thirdhand smoke exposure raises new concerns," *Environmental Health Perspectives*, vol. 119, no. 2, pp. A70–A74, 2011.
- [9] S. Rezapour, C. T. Deressa, and S. Etemad, "On a memristor-based hyperchaotic circuit in the context of nonlocal and non-singular kernel fractional operator," *Journal of Mathematics*, vol. 2021, Article ID 6027246, 21 pages, 2021.
- [10] N. Sarwar, M. I. Asjad, T. Sitthiwiratham, N. Patanarapeelert, and T. Muhammad, "A Prabhakar fractional approach for the convection flow of casson fluid across an oscillating surface based on the generalized Fourier law," *Symmetry*, vol. 13, no. 11, p. 2039, 2021.
- [11] S. Ahmad, A. Ullah, Q. M. Al-Mdallal, H. Khan, K. Shah, and A. Khan, "Fractional order mathematical modeling of COVID-19 transmission," *Solitons & Fractals*, vol. 139, article 110256, 2020.
- [12] P. Kumar, V. S. Erturk, and M. Murillo-Arcila, "A new fractional mathematical modelling of COVID-19 with the availability of vaccine," *Results in Physics*, vol. 24, article 104213, 2021.
- [13] Z. Zhang, A. Zeb, O. F. Egbeelowo, and V. S. Erturk, "Dynamics of a fractional order mathematical model for COVID-19 epidemic," *Advances in Difference Equations*, vol. 2020, no. 1, 2020.
- [14] A. Khan, R. Ikram, A. Din, U. W. Humphries, and A. Akgul, "Stochastic COVID-19 SEIQ epidemic model with time-delay," *Results in Physics*, vol. 30, p. 104775, 2021.
- [15] M. A. Dokuyucu, E. Celik, H. Bulut, and H. M. Baskonus, "Cancer treatment model with the Caputo-Fabrizio fractional derivative," *The European Physical Journal Plus*, vol. 133, no. 3, p. 92, 2018.
- [16] M. El Younoussi, Z. Hajhouji, K. Hattaf, and N. Yousfi, "A new fractional model for cancer therapy with M1 oncolytic virus," *Complexity*, vol. 2021, Article ID 9934070, 12 pages, 2021.
- [17] M. Z. Ullah, A. K. Alzahrani, and D. Baleanu, "An efficient numerical technique for a new fractional tuberculosis model with nonsingular derivative operator," *Journal of Taibah University for Science*, vol. 13, no. 1, pp. 1147–1157, 2019.
- [18] K. Shah, M. A. Alqudah, F. Jarad, and T. Abdeljawad, "Semi-analytical study of Pine Wilt disease model with convex rate under Caputo-Fabrizio fractional order derivative," *Solitons & Fractals*, vol. 135, article 109754, 2020.
- [19] D. Baleanu, S. M. Aydogan, H. Mohammadi, and S. Rezapour, "On modelling of epidemic childhood diseases with the Caputo-Fabrizio derivative by using the Laplace Adomian decomposition method," *Alexandria Engineering Journal*, vol. 59, no. 5, pp. 3029–3039, 2020.
- [20] H. Khan, J. F. Gomez-Aguilar, A. Alkhazzan, and A. Khan, "A fractional order HIV-TB coinfection model with nonsingular Mittag-Leffler law," *Mathematical Methods in the Applied Sciences*, vol. 43, no. 6, pp. 3786–3806, 2020.
- [21] H. Mohammadi, S. Kumar, S. Rezapour, and S. Etemad, "A theoretical study of the Caputo-Fabrizio fractional modeling for hearing loss due to Mumps virus with optimal control," *Solitons & Fractals*, vol. 144, article 110668, 2021.
- [22] M. Jleli and B. Samet, "On the well-posedness of a fractional model of HIV infection," *Journal of Function Spaces*, vol. 2020, Article ID 6617245, 9 pages, 2020.
- [23] S. A. Khan, K. Shah, G. Zaman, and F. Jarad, "Existence theory and numerical solutions to smoking model under Caputo-Fabrizio fractional derivative," *Chaos*, vol. 29, no. 1, article 013128, 2019.
- [24] Z. U. A. Zafar, H. Rezazadeh, M. Inc, K. S. Nisar, T. A. Sulaiman, and A. Yusuf, "Fractional order heroin epidemic dynamics," *Alexandria Engineering Journal*, vol. 60, no. 6, pp. 5157–5165, 2021.
- [25] S. Rezapour, S. Etemad, and H. Mohammadi, "A mathematical analysis of a system of Caputo-Fabrizio fractional differential

- equations for the anthrax disease model in animals,” *Advances in Difference Equations*, vol. 2020, no. 1, 2020.
- [26] J. Singh, D. Kumar, and D. Baleanu, “A new analysis of fractional fish farm model associated with Mittag-Leffler type kernel,” *International Journal of Biomathematics*, vol. 13, no. 2, article 2050010, 2020.
- [27] A. Khan, R. Zarin, U. W. Humphries, A. Akgul, A. Saeed, and T. Gul, “Fractional optimal control of COVID-19 pandemic model with generalized Mittag-Leffler function,” *Advances in difference equations*, vol. 2021, no. 1, 2021.
- [28] A. Akgul, “A novel method for a fractional derivative with non-local and non-singular kernel,” *Solitons Fractals*, vol. 114, pp. 478–482, 2018.
- [29] Z. Alkhudhari, S. Al-Sheikh, and S. Al-Tuwairqi, “Global dynamics of a mathematical model on smoking,” *International Scholarly Research Notices*, vol. 2014, Article ID 847075, 7 pages, 2014.
- [30] V. Verma and M. Agarwal, “Global dynamics of a mathematical model on smoking with media campaigns,” *Research Desk*, vol. 4, pp. 500–512, 2015.
- [31] M. A. Adhana and T. T. Mekonnen, “A mathematical model analysis of smoking tobacco in the case of Haremaya town; Ethiopia,” *International Journal of Research Studies in Science, Engineering and Technology*, vol. 6, no. 2, pp. 14–24, 2019.
- [32] A. M. Pulecio-Montoya, L. E. Lopez-Montenegro, and L. M. Benavides, “Analysis of a mathematical model of smoking,” *Contemporary Engineering Sciences*, vol. 12, no. 3, pp. 117–129, 2019.
- [33] A. Atangana, “Fractal-fractional differentiation and integration: connecting fractal calculus and fractional calculus to predict complex system,” *Solitons & Fractals*, vol. 102, pp. 396–406, 2017.
- [34] J. F. Gomez-Aguilar, T. Cordova-Fraga, T. Abdeljawad, A. Khan, and H. Khan, “Analysis of fractal-fractional malaria transmission model,” *Fractals*, vol. 28, no. 8, article 2040041, 2020.
- [35] K. Shah, M. Arfan, I. Mahariq, A. Ahmadian, S. Salahshour, and M. Ferrara, “Fractal-fractional mathematical model addressing the situation of Corona virus in Pakistan,” *Results in Physics*, vol. 19, article 103560, 2020.
- [36] Z. Ali, F. Rabiei, K. Shah, and T. Khodadadi, “Qualitative analysis of fractal-fractional order COVID-19 mathematical model with case study of Wuhan,” *Alexandria Engineering Journal*, vol. 60, no. 1, pp. 477–489, 2021.
- [37] M. Farman, A. Akgul, K. S. Nisar et al., “Epidemiological analysis of fractional order COVID-19 model with Mittag-Leffler kernel,” *AIMS Mathematics*, vol. 7, no. 1, pp. 756–783, 2021.
- [38] M. Amin, M. Farman, A. Akgul, and R. T. Alqahtani, “Effect of vaccination to control COVID-19 with fractal fractional operator,” *Alexandria Engineering Journal*, vol. 61, no. 5, pp. 3551–3557, 2022.
- [39] M. Alqhtani and K. M. Saad, “Fractal-fractional Michaelis-Menten enzymatic reaction model via different kernels,” *Fractal and Fractional*, vol. 6, no. 1, p. 13, 2022.
- [40] K. M. Saad, M. Alqhtani, and J. F. Gomez-Aguilar, “Fractal-fractional study of the hepatitis C virus infection model,” *Results in Physics*, vol. 19, article 103555, 2020.
- [41] A. Granas and J. Dugundji, *Fixed Point Theory*, Springer-Verlag, New York, 2003.
- [42] D. Gopal and S. Jain, *Metric Structures and Fixed Point Theory: Fixed Point Theory in Partial Metric Spaces*, Chapman and Hall/CRC, 1st Edition edition, 2021.
- [43] V. Joshi and S. Jain, *Metric Structures and Fixed Point Theory: G-Metric Spaces: From the Perspective of F-Contraactions and Best Proximity Points*, Chapman and Hall/CRC, 1st Edition edition, 2021.
- [44] B. Samet, C. Vetro, and P. Vetro, “Fixed point theorems for α - ψ -contractive type mappings,” *Nonlinear Analysis*, vol. 75, no. 4, pp. 2154–2165, 2012.
- [45] B. Fekede and B. Mebrate, “Sensitivity and mathematical model analysis on secondhand smoking tobacco,” *Journal of the Egyptian Mathematical Society*, vol. 28, no. 1, p. 50, 2020.
- [46] S. M. Ulam, *Problems in Modern Mathematics*, Wiley, New York, NY, USA, 1940.
- [47] D. Hyers, “On the stability of the linear functional equation,” *Proceedings of the National Academy of Sciences of the United States of America*, vol. 27, no. 4, pp. 222–224, 1941.
- [48] P. V. D. Driessche and J. Watmough, “Reproduction numbers and sub-threshold endemic equilibria for compartmental models of disease transmission,” *Mathematical Biosciences*, 2002, vol. 180, no. 1-2, pp. 29–48, 2002.
- [49] N. Chitnis, J. M. Hyman, and J. M. Cushing, “Determining important parameters in the spread of malaria through the sensitivity analysis of a mathematical model,” *Bulletin of Mathematical Biology*, vol. 70, no. 5, pp. 1272–1296, 2008.
- [50] M. Toufik and A. Atangana, “New numerical approximation of fractional derivative with non-local and non-singular kernel: application to chaotic models,” *The European Physical Journal Plus*, vol. 132, no. 10, p. 444, 2017.